Effect of carbonation on bacteria-based self-healing of cementitious composites

Linzhen Tan[a], Bianca Reeksting[b], Veronica Ferrandiz-Mas[a], Andrew Heath[a], Susanne Gebhard[b] and Kevin Paine[a]

[a] BRE Centre for Innovative Construction Materials, University of Bath, UK

[b] Department of Biology and Biochemistry, Milner Centre for Evolution, University of Bath, UK

Corresponding author:

Kevin Paine

BRE Centre for Innovative Construction Materials

University of Bath, UK

BA2 7AY

k.paine@bath.ac.uk

ABSTRACT

Self-healing cementitious composites are being developed to respond to the high cost of repair and maintenance of infrastructure. A promising solution is the use of bacteria to induce calcium carbonate precipitation within cracks when they occur and prevent further deterioration. Previous work has shown successful bacteria-mediated self-healing of cementitious composites at early-ages, in conditions where the material was uncarbonated prior to cracking. However, as cementitious composites often crack when they have reached a more aged state and are likely carbonated at the time of crack formation, these previous experiments did not fully reflect the real-world situation. In the present study, we show that for cementitious composites that do not carbonate prior to cracking the calcium hydroxide created as a hydration product is a sufficient source of Ca^{2+} ions to provide effective bacteria-induced healing. We note that supplying an extra source of Ca^{2+} ions at the moment of cracking, delivered via encapsulation, further enhances the degree of healing. Importantly however, in carbonated mortars calcium hydroxide is not available as a source of Ca^{2+} ions. Consequently, we show for the first time that bacteria-based self-healing in mortars that have carbonated prior to cracking is almost totally dependent on the availability of Ca^{2+} ions released from an encapsulated source. Our study therefore provides important insights for the rational design of self-healing concrete, where the conditions of the concrete during service life need to be taken into consideration when choosing between direct addition or encapsulation of calcium sources to ensure optimal performance.

Keywords: cracking; carbonation; self-healing; bacteria; concrete; mortar

1. INTRODUCTION

Concrete dominates our built infrastructure due to its reliable strength, durability, versatility and thermal mass. However, concrete is relatively weak in tension and invariably cracks in service. These cracks can act as pathways for the ingress of deleterious substances, which may impair structural performance by instigating chemical attack on the reinforcing steel or the cementitious matrix itself. It has been calculated that within the UK the annual cost of repairing our infrastructure (mainly concrete) is £40bn, and the cost of disruption may be an order of magnitude higher again [1]. As an alternative to repair, there has been much interest in developing concretes and other cementitious composites that are able to self-heal their own cracks and consequently reduce or even eliminate maintenance costs.

A number of techniques to provide self-healing in cementitious composites have been described in recent years, including stimulated autogenous methods (for example, superabsorbent polymers [2] and crystalline admixtures [3] that accelerate the formation of cementitious hydration products on the surfaces of the crack), and autonomic approaches (using minerals or polymers in an encapsulated form [4,5] or via vascular networks [6]) that release materials that hydrate or harden to fill the crack. These and other approaches have been described in detailed state-of-the-art reports [1,7].

A further autonomic approach is to utilise microbiologically induced calcite precipitates as a healing product. This can be achieved by embedding spores of appropriate bacteria within the concrete alongside nutrients to promote their growth. When a crack forms and water and oxygen ingress, the spores germinate into active cells. In an environment rich in dissolved inorganic carbon (DIC) and Ca^{2+} ions the bacteria aid and accelerate the precipitation of calcium carbonate, usually as calcite, within cracks [8–11]. There are a number of pathways by which bacteria may precipitate calcium carbonate [12,13], but they all generally require: (i) a sufficient concentration of DIC within the pore water within the vicinity of the crack to enable formation of CO_3^{2-} ions, (ii) a change in local pH; (iii) attraction of Ca^{2+} ions to the

66 negatively charged surface of the bacteria, where the bacteria may act as a nucleation point;
67 and (iv) a sufficient quantity of Ca^{2+} to precipitate calcium carbonate.
68 The ability of bacteria to autonomously heal cracks in cementitious composites by
69 precipitating calcium carbonate has been verified in several studies using a number of
70 technologies [14–21]. Since both Ca^{2+} and CO_3^{2-} ions are required, technologies have been
71 developed that provide these as separate additions (e.g. urea plus calcium nitrate), or by the
72 use of organic calcium salts (e.g. calcium lactate) which supplies both in a single additive.
73 Although the precise source of Ca^{2+} ions used by the bacteria during self-healing is unclear,
74 it has been proposed that calcium hydroxide is likely to be the most important source [22].
75 Therefore, it is interesting to note that in all previous studies, self-healing of the cracks has
76 been tested on water-cured mortars or concretes at a relatively young age (~28 days) where
77 calcium hydroxide is present as a hydration product and provides a plentiful supply of
78 soluble Ca^{2+} ions. Thus, it has been questioned to what extent the addition of further Ca^{2+}
79 ions is necessary [23].
80 That said, in many real-life environments, particularly those where the concrete is subject to
81 alternate wetting and drying, a process of carbonation can occur before the concrete cracks.
82 Here, environmental CO_2 dissolved in pore water accesses the concrete and, through a
83 series of reactions, calcium hydroxide is converted to calcium carbonate. The outcome is
84 that Ca^{2+} ions become trapped in a less soluble form [24]. Since there is no evidence that
85 bacteria can utilise the Ca^{2+} ions in calcium carbonate, there is a concern that bacteria-
86 based self-healing may not occur in concrete that has carbonated before cracking.
87 Furthermore, the quantity of CO_3^{2-} ions available for self-healing is related to the
88 concentration of DIC in the vicinity of the crack when it occurs. Whilst this may be
89 supplemented by the use of urea ($CO_2(NH_2)_2$) or organic salts, it should be noted that yeast
90 extract is nearly always used as an addition to bacteria-based cementitious composites to
91 promote germination of the spores and growth of the cells. Yeast extract contains carbon,

and it is likely that its metabolic breakdown provides a sufficient source of DIC. However, this has not yet been proven.

The research described in this paper was carried out to ascertain for the first time whether:

1. Self-healing occurs in mortar that has carbonated prior to cracking; when: (i) the calcium source is added directly to the concrete mix and (ii) when the calcium source is encapsulated.
2. Yeast extract could be used as the sole added source of DIC, thus eliminating the need for urea and organic salts and consequently simplifying mix designs.

For reasons of scale, the work carried out in this paper, as in other leading studies on self-healing cementitious composites [9,21,25], has been performed on mortars where the maximum aggregate size is ~4 mm. However, given that the cracks in concrete generally form and propagate in the mortar phase, the results of this work are equally applicable to self-healing of concrete and other cementitious composites.

2. MATERIALS AND METHODS

2.1 Bacterial Strain

The alkaliphilic species *Bacillus cohnii* DSM 6307 was obtained from the German Collection of Microorganisms and Cell Culture (DSMZ), Braunschweig, Germany. They were stored in 50% (v/v) glycerol at -80 °C. To routinely culture *B. cohnii*, lysogeny broth (LB) was mixed with alkaline solution (10% v/v) which contained 100 ml/l Na-sesquicarbonate (42 g/l $NaHCO_3$ and 53 g/l Na_2CO_3 anhydrous) to adjust to pH 9.5.

Bacterial spores were grown in sporulation medium and harvested after 48 hours by centrifugation [26]. Spores were collected by centrifugation at 3800 x *g* for 10 minutes, and the spore pellet was washed thrice with chilled 10 mmol/l Tris-HCl buffer pH 9. Chlorohexidine digluconate (0.3 mg/ml) was applied afterwards to kill vegetative cells followed by a further three washes with the same Tris-HCl buffer. Spore pellets were snap-frozen in liquid nitrogen and freeze-dried under vacuum overnight. Viability of spores (colony forming units (cfu) per gram dry weight) was determined by dilution plating.

2.2 Growth Media

The growth media (GM) used in this study was comprised of calcium nitrate and yeast extract. Both calcium nitrate and yeast extract were supplied by Sigma-Aldrich Corporation. The GM were either adding directly into mortar matrix or encapsulated in lightweight aerated concrete granules (ACG).

2.3 Aerated concrete granules

The ACG used were a commercially available product supplied by Cellumat SA Belgium. They were used as the porous media for immobilisation of the spores, and as a carrier for calcium nitrate and yeast extract in selected mixes. The ACG, as supplied, were separated to produce a particle size distribution conforming to a 0/4 mm aggregate as defined in BS EN 12620. The ACG, as used, had a water absorption capacity of 120% and a loose dry bulk density of 354 kg/m^3.

2.4 Encapsulation Process

Both the bacterial spores and GM were encapsulated in ACG under vacuum. The procedures were done independently to create ACG containing spores and ACG containing GM. The method for vacuum impregnation was based on that described by Alghamri *et al* [27]. A vacuum chamber with two-entry valves was set up as shown in Figure 1. One valve was connected to a reservoir containing a suspension of spores or a solution of GM, whilst the second valve was connected to the vacuum channel at 0.8 bar. For ACG containing spores, a batch was made by resuspending spores (12.5 x 10^{10} cfu) in 10 ml distilled water which was then imbibed into 18 g ACG. For ACG containing GM, the GM (4.55 g calcium nitrate and 1 g (or 4g) of yeast extract) was dissolved in distilled water before being imbibed into the ACG. The amount of distilled water within the suspension or solution equalled the

total water absorption capacity of ACG ensuring that the ACG were entirely saturated after encapsulation.

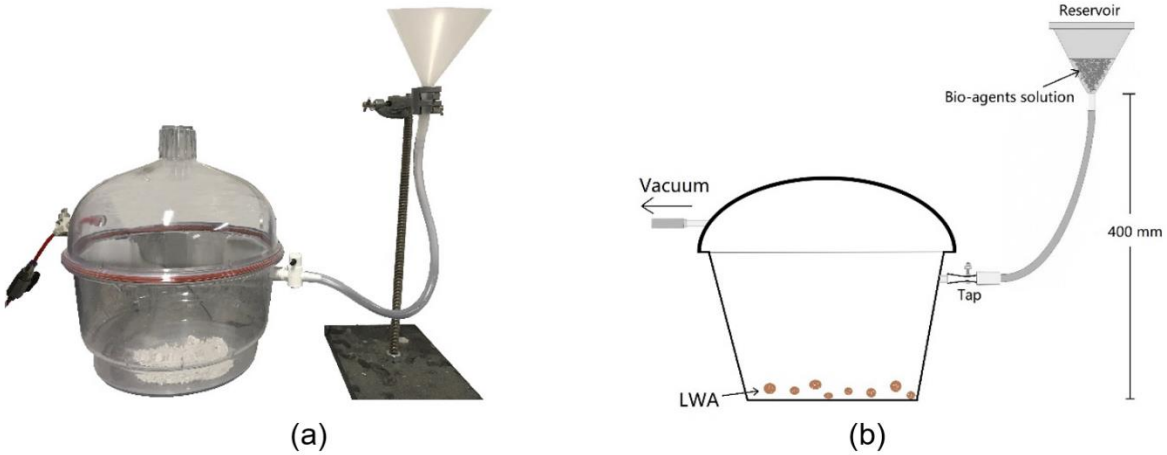

Figure 1 Vacuum encapsulation set-up, (a) on site, (b) schematic

After the encapsulation process, the ACG were placed in an environmental chamber at 50% relative humidity and 20°C for 24 hours to obtain a dry surface. Following this the ACG were coated with PVA (polyvinyl acetate), supplied by BOSTIK Ltd, to provide a waterproof protective layer. To achieve an even distribution of coating on the ACG, a Kenwood Major Titanium Mixer with a K-Blade was utilized. Mixing proceeded until PVA was slightly dried on the surface of ACG in case of any adhesive between particles. Thereafter, the coated ACG containing spores (ACGS) and coated granules containing GM (ACGM) were stored in air-tight plastic bags until used in mortar mixes.

The mass of the coating for ACGS and ACGM was approximately 33% of the overall mass of the coated ACG and consequently the number of spores was approximately 6.9×10^9 spores per g of coated ACG. Less than 6% of coated particles by mass passed a 2 mm sieve, compared with approximately 35% by mass passing this sieve prior to coating.

2.5 Preparation of mortar specimens

A series of mortars were produced using Portland limestone cement (CEM II/A-L 32.5R), standard sand conforming to BS EN 196-1, tap water and (i) ACGS and ACGM, or (ii) GM directly added to the mortar matrix (without encapsulation). The mix proportions are given in Table 1. The reference mortar (REF) was a standard cement mortar mix with water to cement ratio of 0.5 conforming to BS EN 196-1. A control mortar (CTRL) was made to assess the effect of the direct addition of growth media (4.55g calcium nitrate and 1g yeast extract) on the performance but without the addition of any spores.

The final three mortars (CaN-direct, CaN-encap and CaNY-encap) all contained spores in the form of the addition of 5.25 g of ACGS – approximating to 3.64×10^{10} spores. For CaN-direct mix, the growth media were added directly to the mortar as per CTRL. For CaN-encap, the growth media was added in the form of 22 g of ACGM (which equalled the addition of 4.55 g calcium nitrate and 1 g yeast extract). For the final mortar, CaNY-encap, the ACGM contained 4.55 g of calcium nitrate and 4 g of yeast extract, i.e. it had a higher quantity of yeast extract.

Table 1 Mix proportions for all mortar samples

Specimens	Cement (g)	Water (g)	Standard sand(g)	Yeast extract(g)	Calcium nitrate(g)	ACGS (g)	ACGM (g)
REF	92	46	276	0	0	0	0
CTRL	92	46	276	1	4.55	0	0
CaN-direct	92	46	260	1	4.55	5.25	0
CaN-encap	92	46	207	0	0	5.25	22.0 (contains 4.55 g calcium nitrate, 1 g yeast extract)
CaNY-encap	92	46	207	0	0	5.25	25.0 (contains 4.55 g calcium nitrate, 4 g yeast extract)

Mixing was carried out in accordance with BS EN 196-1 with the ACGS and ACGM added at the same time as the sand. Mortars were cast into prisms of dimension 65 mm × 40 mm × 40 mm. Specimens were comprised of two layers. To conserve spores, only the lower layer (20 mm deep) was self-healing mortar (as per the proportions in Table 1), whilst the upper layer (20 mm) contained REF mortar. The lower layer was cast first. After approximately 60

minutes the upper layer was then cast on top. After casting, the specimens were cured in a controlled environment room (20°C, 40% RH) for 24 hours and then demoulded. After demoulding, they were cured under water at 20°C. Specimens to be tested in an uncarbonated condition were cured in water until an age of 28 days, whilst those to be carbonated were removed from water at an age of 14 days and placed in a carbonation chamber for a further 28 days.

To determine the effect of carbonation on the hydration products, particularly the mass of calcium hydroxide and calcium carbonate, thermogravimetric analysis (TGA) and X-ray powder diffraction (XRD) were carried out on paste samples. All pastes matched the mix ratios given in Table 1 subject to the elimination of the sand. Duplicate paste samples were made with one cured in water and the other subject to the carbonation regime.

2.6 Test methods

2.6.1 Isothermal conduction calorimetry

To investigate the effect of self-healing agents on the hydration of cement, isothermal conduction calorimetry tests were conducted using a Calmetrix I-cal 4000. All tests were carried out on mortar samples at 20°C. Mix proportions of mortar samples were in the same proportions as given in Table 1.

2.6.2 Carbonation

After 14 days of curing, selected mortar and paste specimens were placed in a carbonation chamber with a CO_2 concentration of 20% and relative humidity of 50% for 28 days. To evaluate the effectiveness of the carbonation method, thermogravimetric analysis (TGA) was carried out using a Setsys Evolution TGA 16/18 instrument on the hardened pastes. 20 mg of hardened paste was placed in an alumina crucible and heated from 30 to 1000°C at a rate of 10°C/minute under 50 ml/minute flow of inert nitrogen gas.

2.6.3 Crack creation

After 28 days the specimens were dried at room temperature for 24 hours. The top third of the prims was wrapped with carbon fibre reinforced polymer strips to enable a controlled width crack to be generated. Specimens were subjected to cracking using three-point bending using a 30 kN Instron static testing frame over a span of 60 mm with the load applied at the centre point (Figure 2(a)) to generate a crack through the lower part of the prisms containing the healing agents. Crack opening was measured using a crack mouth opening displacement (CMOD) gauge. A notch of approximately 1.5 mm depth was sawn at mid-span to serve as an initiation point to cracking. Load was applied to maintain a crack growth of 20 μm per minute. Loading was stopped when the crack width was sufficiently large (~ 1 mm) that it could be expected to be approximately 500 μm wide on removal of the load after allowing for elastic rebound. Selected parts of the crack were marked with a permanent marker pen (Figure. 2(b)) to facilitate the monitoring of crack healing using an optical microscope.

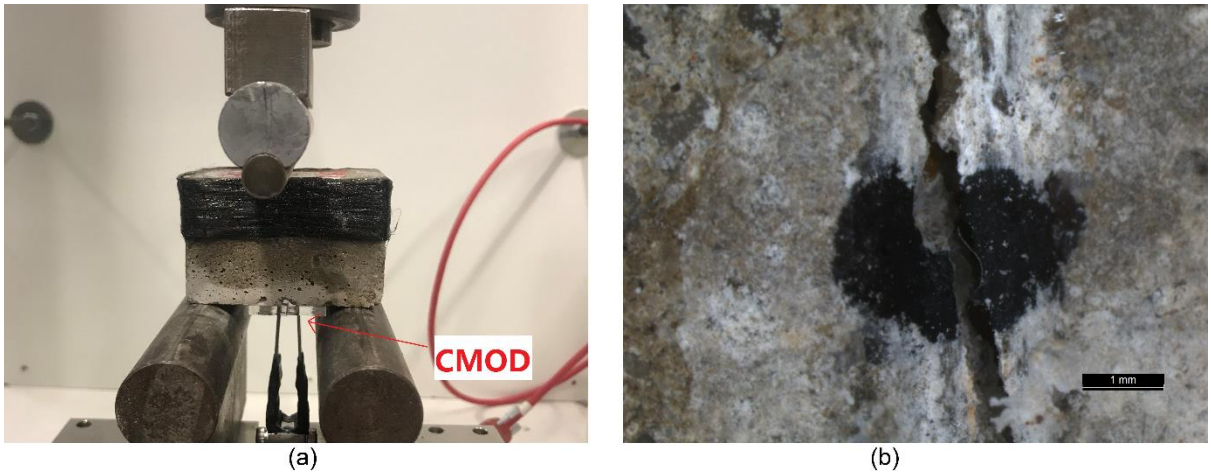

(a) (b)

Figure 2 Creation of cracks in hardened mortar, (a) three-point bending set-up, (b) marked crack

2.6.4 Healing

Following cracking, all prisms were subjected to the healing regime. Prisms were placed in a plastic tank container and supported 10 mm above the base to permit water to flow around all sides. The tank was kept open to the atmosphere during the incubation period at 20°C. A

wet-dry cycle of 16 hours wet and 8 hours dry was used. The system used is shown in Figure 3, in which two external pumps automatically released water from the lower tank (during the wetting period) and drained water from the upper tank during the drying period.

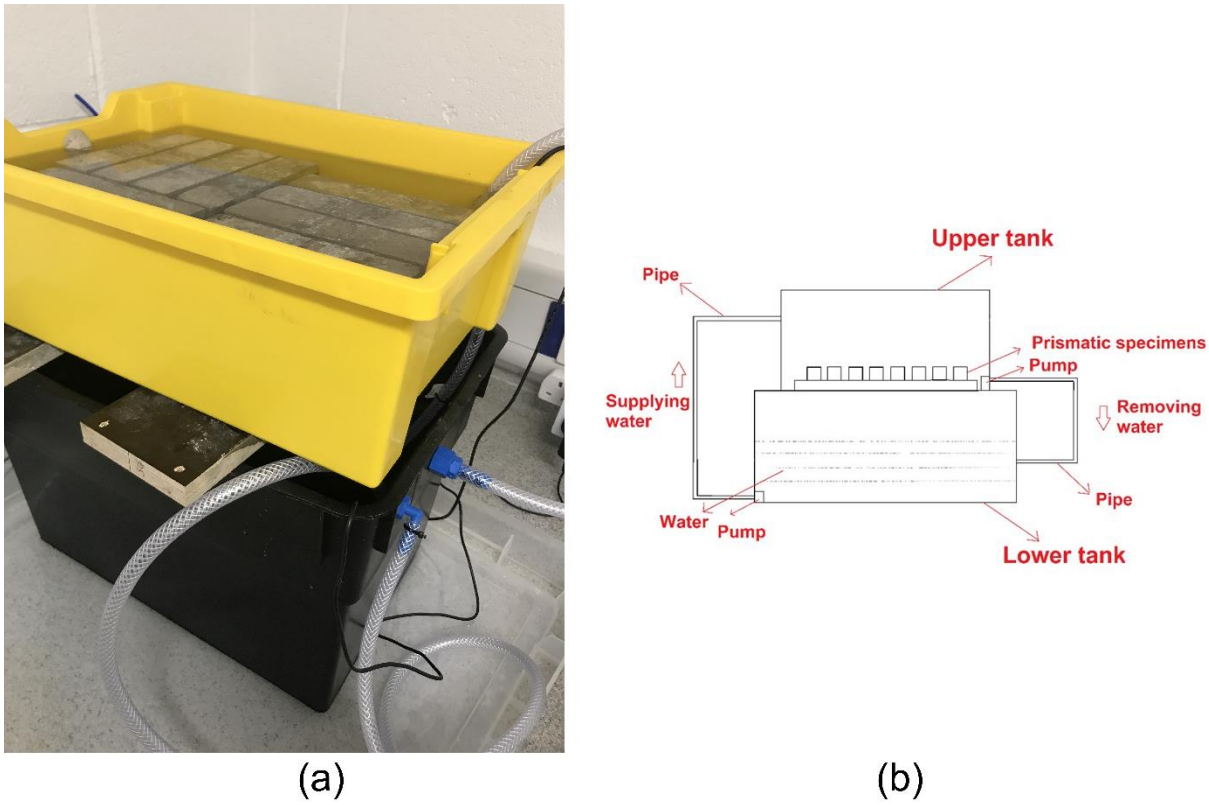

Figure 3 Wet-dry healing regime, (a) on site, (b) schematic image

2.6.5 Investigation of self-healing efficiency

Visualisation of crack-filling

Visualisation of crack filling was performed using a Leica M205C light microscope. Images were taken of freshly cracked samples after 7, 14, 28, 56 and 84 days of healing to determine the crack width. The same part of the crack was observed every time.

Healing ratios (R_W) were calculated based on Equation 1:

$$R_W = \frac{W_0 - W_1}{W_0} \times 100\% \qquad \text{Equation 1}$$

where W_0 was the initial crack width immediately after cracking and W_1 was the crack width after healing.

Water flow

The progressive improvement in water-resisting properties of the mortar as the crack healed was determined using a water-flow test. Tests were carried out immediately after cracking and after 28 days of healing. The water-flow test was based on RILEM Test Method 11.4 [28]. The set-up of the water-flow test is shown in Figure 4, and the water-flow coefficient, K, was calculated by Equation 2 [29].

$$K = \frac{aL}{At} \ln\left[\frac{h_1}{h_2}\right] \quad \text{Equation 2}$$

Where K is the water-flowing coefficient (cm/s); a is the cross-sectional area of the pipette (cm^2). L is the thickness of specimen (cm); A is the cross-sectional area of specimen which equals the cross-sectional area of acrylic plate (cm^2); t is the time (s); h_1 is the initial water head (cm); h_2 is the final water head (cm).

Healing ratios (R_K) were calculated based on Equation 3:

$$R_K = \frac{K_0 - K_1}{K_0} \times 100\% \quad \text{Equation 3}$$

where K_0 was the water flow coefficient after cracking and K_1 was the water flow coefficient after healing.

2.6.6 Analytic investigation

Selected and representative specimens were visualised under a scanning electron microscope (SEM) after 90 days healing. These were placed in a E306 Edward Vacuum Coating System until samples had outgassed. A Jeol JSM-6480LV scanning electron

microscope was used to obtain the image, and a backscattered image technique was used at 10 kV, in which images were obtained in low vacuum and no coating was required. Energy dispersive X-ray detection (EDX) was conducted at the same time as SEM to detect the element composition of the healing product. A comparative element analysis was conducted on the surface more than 15 mm from the crack, to aid in identification of the differences between healing products and the cement hydration products.

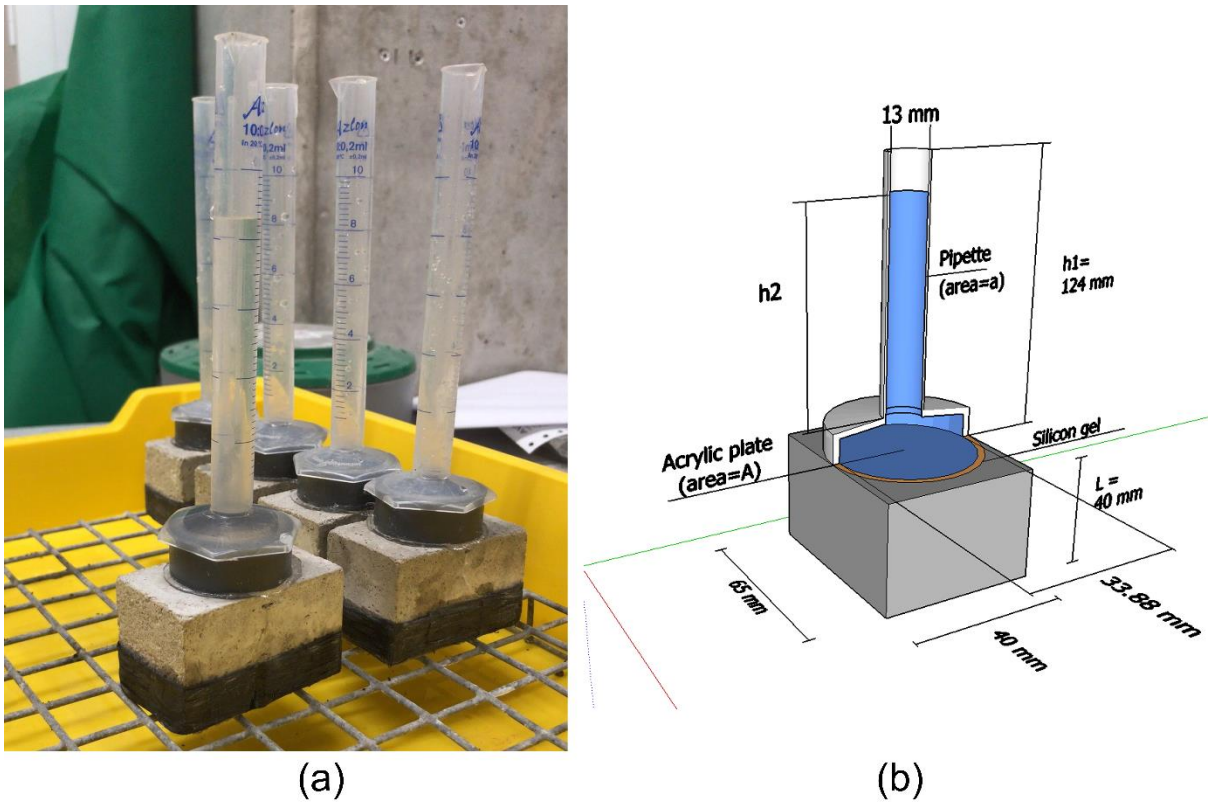

Figure 4 Water flow test, (a) on site set-up, (b) schematic image

3. RESULTS

3.1 Kinetics of hydration

The kinetics of hydration of the five pastes are shown in Figure 5(a). The REF paste showed typical behaviour of a CEM II/L-A paste and had a maximum rate of heat production at around seven hours and a small secondary peak at approximately 10 hours. For the CTRL paste, where calcium nitrate and yeast extract were added directly, a substantial delay in hydration was seen, with a much longer dormant period and the maximum rate of heat production occurring as late as 20 hours after the addition of water to the cement. For CaN-direct paste, where the only difference to the CTRL paste was the addition of encapsulated spores, a similar trend was recorded. These delays in hydration are most likely due to the inclusion of the yeast extract and the presence of sugars, as has been noted elsewhere [30,31].

However, in the two pastes where calcium nitrate and yeast extract were encapsulated in ACG prior to adding them to the paste (CaN-encap or CaNY-encap), there was no noticeable delay in hydration. Both of these samples had maximum rates of heat production at around seven hours, the same as the REF paste. From this it can be concluded that the encapsulation of the GM in ACG and then coating this with PVA was sufficient to prevent leaching of GM during mixing. However, it should be noted that the maximum rate of heat production was smaller at approximately 1.5 mW/g compared to 2.9 mW/g for the REF paste. It is not clear why this was the case.

Figure 5(b) shows the cumulative heat production. Although the CTRL and CaN-direct pastes were retarded, the total heat produced at around 72 hours was similar to the REF paste suggesting that similar levels of cement hydration have been achieved. Overall, CaNY-encap had the lowest total heat at 72 hours.

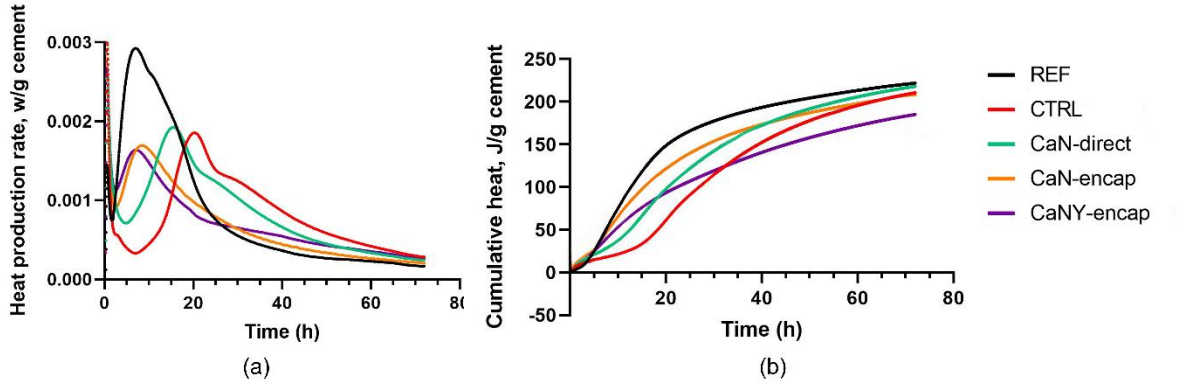

313

314 *Figure 5 Kinetics of hydration, (a) heat production rate, (b) cumulative heat*

315

316 **3.2 Carbonation**

317 Thermal gravimetric analyses (TGA) and differential thermal gravimetric analysis (dTG) of
318 the REF and CTRL pastes before and after carbonation are shown in Figure 6. The figures
319 show three main troughs: Trough 1 is associated with loss of water attached to hydration
320 products and gypsum, trough 2 is associated with the decomposition of calcium hydroxide to
321 CaO and H_2O, whilst trough 3 is primarily related to the decomposition of calcium carbonate
322 to CaO and CO_2. From the TGA curves it can be calculated that, at 28 days, the calcium
323 hydroxide content of the REF paste was approximately 5% by mass, and that after
324 carbonation it was approximately zero. For the CTRL paste, the calcium hydroxide was 20%
325 by mass in the uncarbonated form (reflecting the direct addition of calcium nitrate and its
326 dissolution to form calcium hydroxide), but again no calcium hydroxide was recorded after
327 carbonation.
328 XRD was carried out on selected specimens before and after carbonation. The results are
329 available in supplementary material. Overall, these results confirmed that the carbonation
330 regime was particularly aggressive and consequently the resulting carbonated mortars were
331 equivalent to mature mortars that have been exposed to XC3/XC4 environments.

332

333

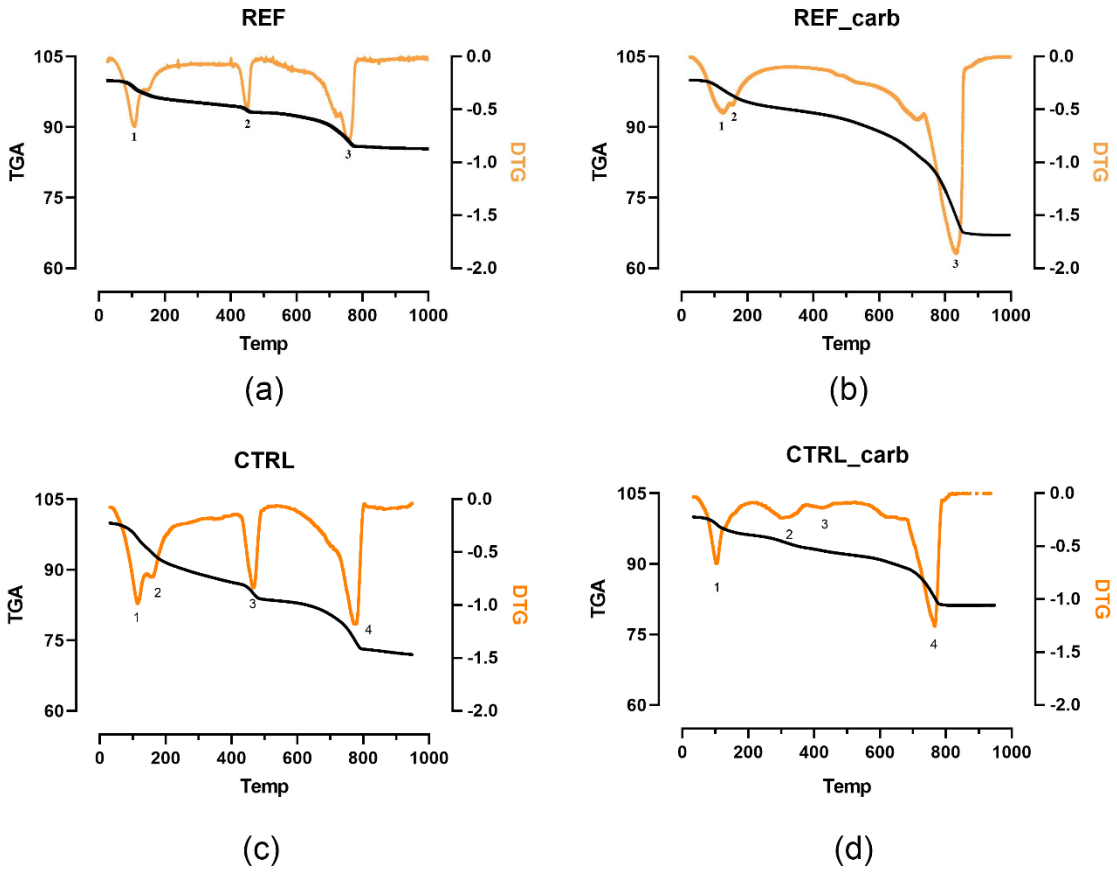

Figure 6 TGA and DTG results of (a) REF, (b) carbonated REF, (c) CTRL and (d) carbonated CTRL pastes

3.4 Healing

3.4.1 Crack closure

The crack size of each mortar was measured using a microscope immediately after cracking and then after 7, 14, 28, 56 and 84 days of healing. The mean initial and final crack widths (84-days) are given in Table 2. Figure 7 shows the crack closure (healing) in terms of the healing ratio (R_w) with time.

Based on the crack size results, the bacteria-based specimens (except for CaN-encap) showed greater overall healing for both uncarbonated and carbonated specimens. Uncarbonated CaN-direct showed a higher degree of crack closure than CaN-encap. The opposite trend was seen in carbonated samples, with the CaN-encap and CaNY-encap having higher healing ratios that CaN-direct. CaNY-encap performed the best in carbonated samples, with a healing ratio of 76%. This suggests that the additional yeast extract contributed to the

self-healing in these specimens. While the smaller initial crack size (0.21 mm) in the CTRL specimen may have facilitated autogenous healing, the degree of healing observed in this sample was still less than that seen in all specimens containing bacteria.

Table 2 Mean values of initial (Wo) and final crack size of all mortars and healing ratio (RW)

Specimens	Uncarbonated			Carbonated		
	Initial crack size (mm)	84-days healed crack size (mm)	Healing ratio (%)	Initial crack size (mm)	84-days healed crack size (mm)	Healing ratio (%)
REF	0.38	0.38	0	0.49	0.49	0
CTRL	0.21	0.04	80%	0.35	0.35	0
CaN-direct	0.52	0.01	98%	0.38	0.32	15%
CaN-encap	0.52	0.10	81%	0.36	0.24	33%
CaNY-encap	0.43	0.00	100%	0.35	0.09	76%

In addition to determining crack widths, crack closure was monitored visually over 84 days of healing using an optical microscope. Figure 8 shows the initial and final appearance (after 84 days) of each mortar for both uncarbonated and carbonated conditions.

In uncarbonated mortars, the REF mortars showed no crystal formation within the crack, which suggested that no autogenous healing took place. On the other hand, the CTRL mortars appeared to be almost completely closed after 28 days. Reasons for this are discussed later.

The mortars containing bacteria showed more rapid healing. CaN-direct presented rapid precipitation on both faces of the crack after 14 days, while CaN-encap and CaNY-encap showed complete crack closure after 7 days. The healing products in mortars that were uncarbonated prior to cracking presented a consistent morphology of large and white crystals.

In carbonated mortars, the REF and CTRL mortars showed no evidence of self-healing. Whilst a few crystals were observed on the crack face of CaN-direct mortars, crack closure was minimal. For the CaN-encap mortar, some transparent thread-like products formed in the crack in the first 56 days, but again crack closure was low (33%). However, for the CaNY-encap mortar translucent, gel-like products formed within the crack. These products

formed quicker than those of CaN-encap, and the degree of crack closure was significant (76%). Cracks in the CaNY-encap mortar were shown to be completely covered by the gel-substance after 28-days healing. However, after 84 days the gel-substance disappeared and crystal precipitates were present within the crack, maintaining the degree of crack closure.

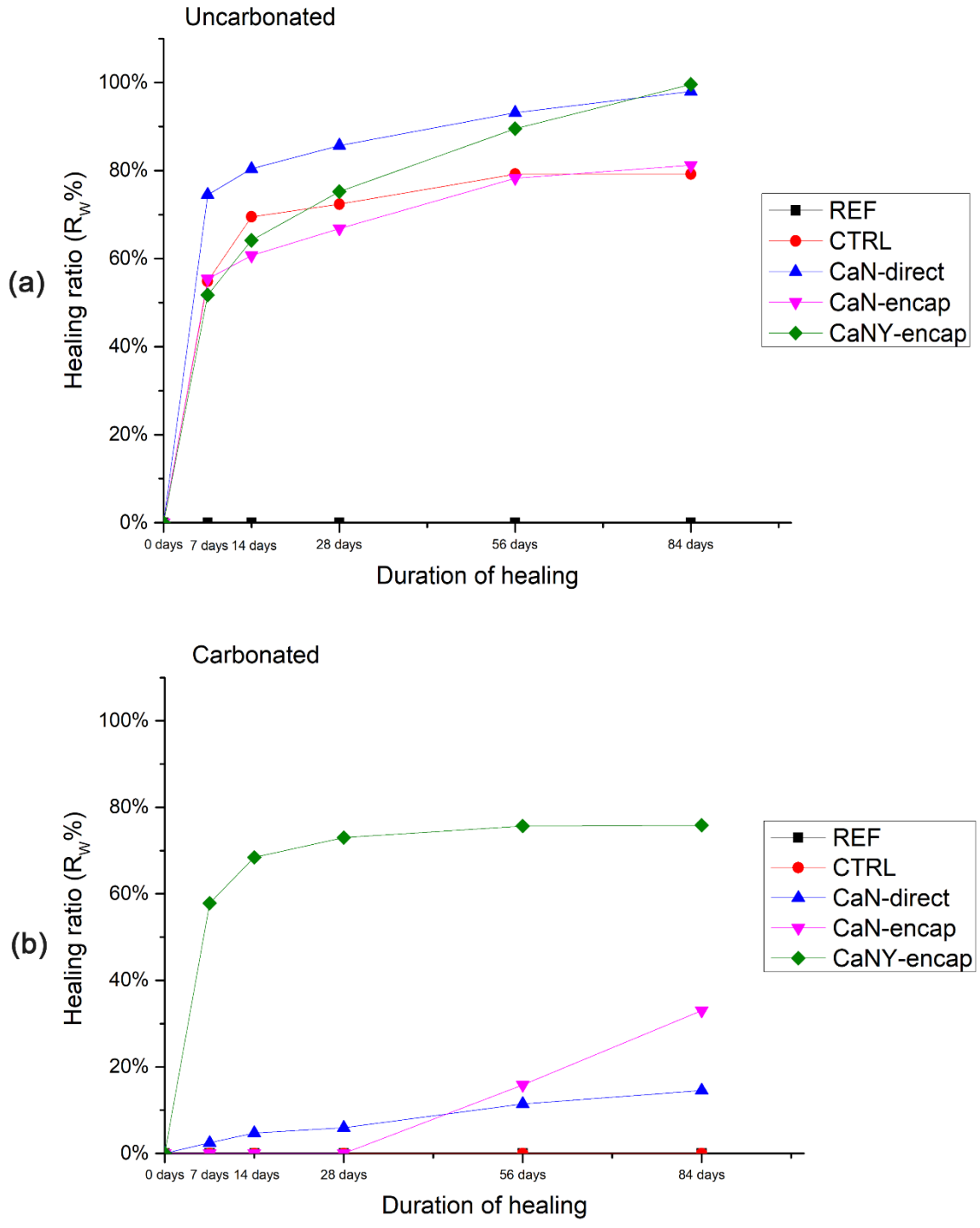

Figure 7 Crack width healing for (a) uncarbonated mortars and (b) carbonated mortars

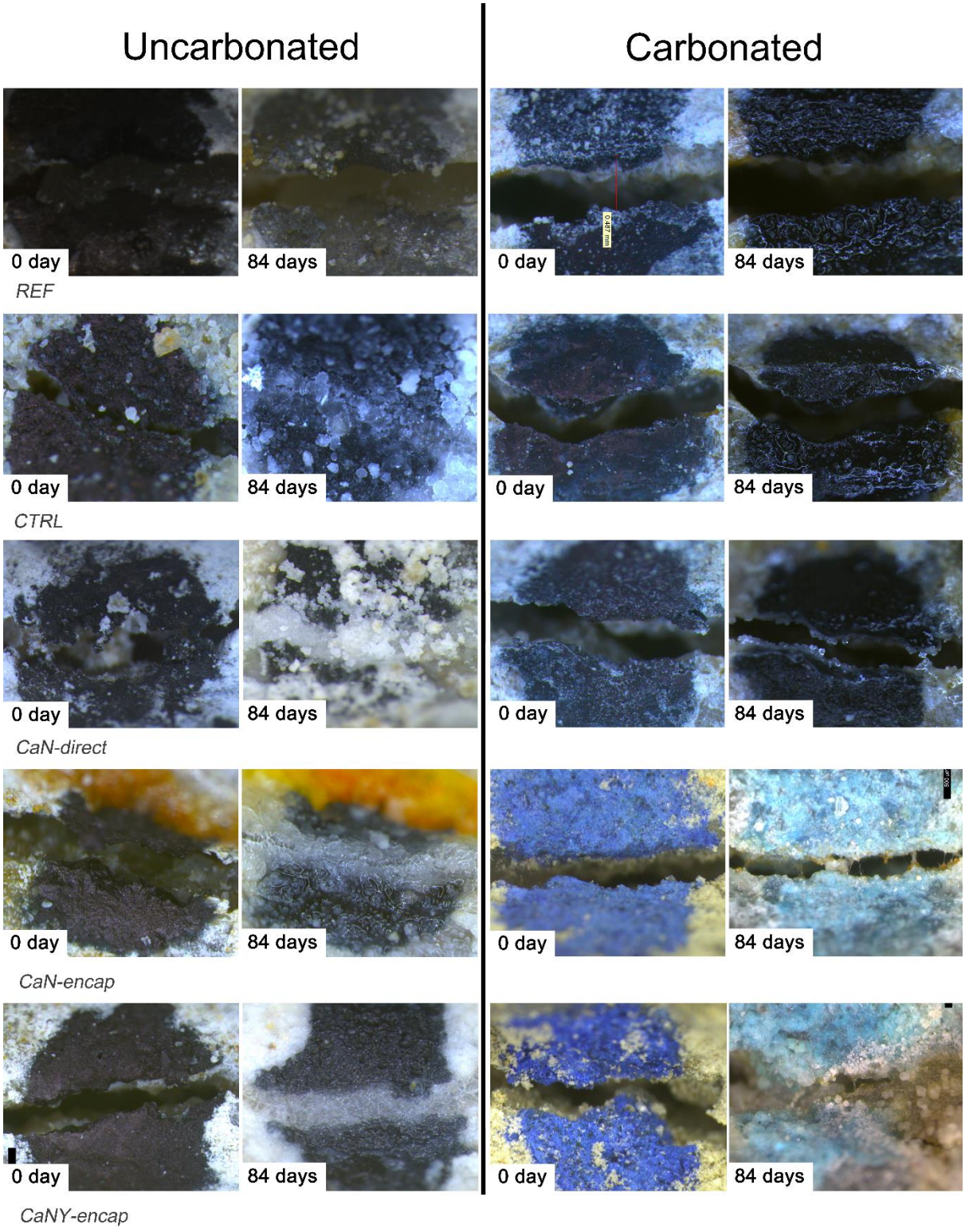

379

380 *Figure 8 Progression of crack healing in images of each mortar*

381

3.4.2 Water flow

Water flow tests were conducted in parallel to the optical microscopy to determine the water movement through the mortars as an indication of how effectively the healing mitigated migration of aggressive substances through the cracked surface. Tests during the healing period were conducted at 28, 56 and 84 days. Initial water flow upon cracking and final water flow after 84 days of healing are given in Table 3. The healing ratio of each mortar compared to the water-flow is shown in Figure 9. These results were generally consistent with the microscopy and measurements of crack closure.

For the uncarbonated mortars (Figure 9a), REF showed only a slight decrease in water flow coefficient after healing (from 0.056 cm/s to 0.036 cm/s), whereas other mortars showed significant reductions in water flow coefficient and therefore higher R_K values. CaNY-encap gave the highest reduction in water flow, followed by CaN-direct. It was noted that the CTRL specimen gave better resistance to water flow after healing than CaN-encap, despite having similar levels of crack width closure (Rw ≈ 80%). This is most likely due to the much lower average crack width of the CTRL mortars such that after 80% crack closure CTRL mortars had an average crack width of 0.04 mm compared to 0.10 mm wide in CaN-encap.

For the carbonated specimens, the REF, CTRL and CaN-direct mortars did not show any significant reduction in water flow after the healing period (Figure 9b). However, the encapsulated specimens showed a different trend, which was consistent with crack closure. The carbonated CaN-encap mortars had a healing ratio of 60% after 28 days, which fell to around 50% at 84 days. For CaNY-encap mortars the healing ratio was over 90% at 28 days and this was maintained at 84 days.

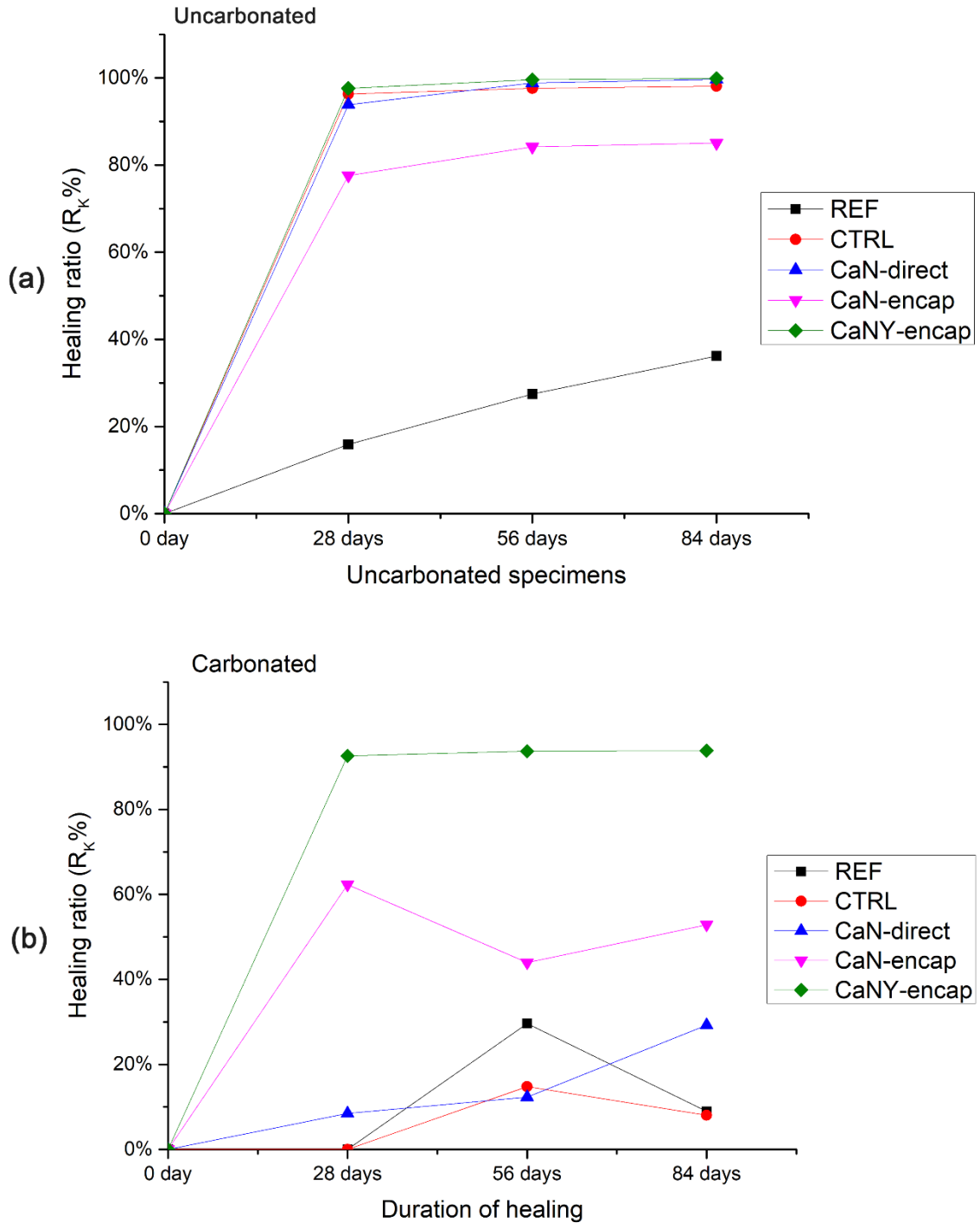

406

407

408 *Figure 9 Healing of mortars in terms of reduction in water-flow coefficient for (a) uncarbonated mortars and (b)*
409 *carbonated mortars*

410

411

412

413 Table 3 Mean values of initial and final water permeability coefficient of specimens

Specimens	Uncarbonated			Carbonated		
	Initial water permeability (cm/s)	Final water permeability (cm/s)	Healing ratio (R_P%)	Initial water permeability (cm/s)	Final water permeability (cm/s)	Healing ratio (R_P%)
REF	0.056	0.036	36%	0.324	0.295	9%
CTRL	0.033	0.001	98%	0.149	0.137	8%
CaN-direct	0.046	0.000	100%	0.130	0.092	29%
CaN-encap	0.244	0.004	85%	0.057	0.027	53%
CaNY-encap	0.140	0.000	100%	0.022	0.001	94%

414

415

416 ***3.4.3 SEM and EDX of healing products***

417 After 90 days of healing, SEM and EDX were conducted on selected mortars. Figure 10
418 shows element mapping analysis as applied to a cracked area of a CaNY-encap mortar. The
419 original mortar is seen at the top and bottom Figure 10(a), and the crack runs through the
420 centre from left to right. In general, the element mapping (Figures 10(b) to Figure 10(d))
421 showed that the healing product contained patches of calcium products present within the
422 crack, but seemingly not necessarily attached to the crack face. Due to the nature of the
423 technique the values for carbon and oxygen are of limited practical application, but it does
424 appear that the crack contains these elements. It can be suggested that the healing product
425 is calcium carbonate. Images on other mortars are given in the supplementary information.

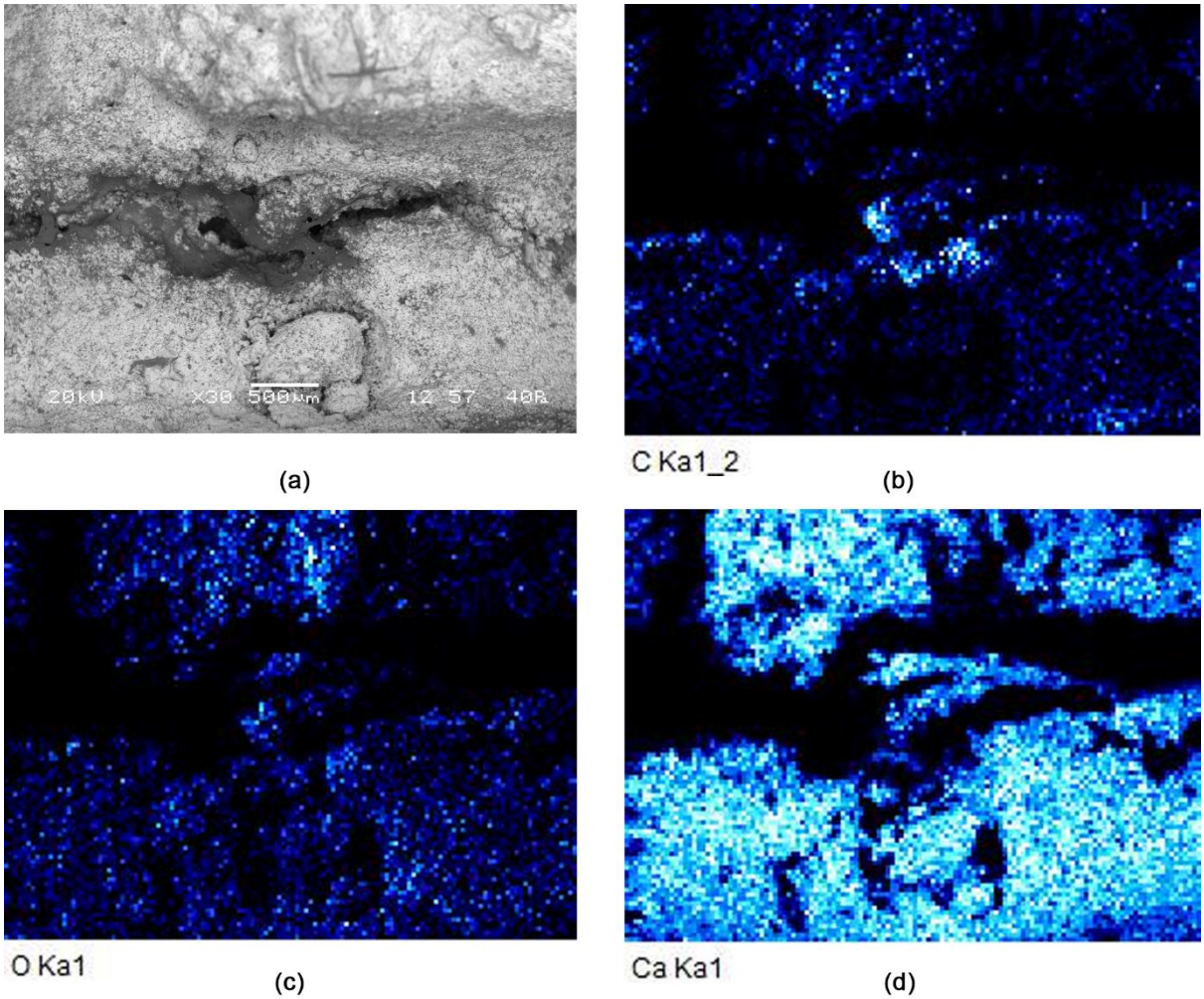

Figure 10 EDX map of carbonated CaNY-encap, (a) applied area, (b) carbon distribution, (c) oxygen distribution and (d) calcium distribution

4. Discussion

4.1 Comparison of healing in uncarbonated and carbonated mortars

4.1.1 Mortars without bacteria

The REF mortars were made with cement and sand, and no additional components. Visual observations showed no healing of the REF mortars for either the uncarbonated or carbonated conditions. This observation shows that the mortars were sufficiently hydrated after 28 days and that no autogenous healing could take place at the surface. The small recovery in water penetration may represent some autogenous healing deep within the crack. The inability of autogenous healing to occur at the surface in the REF mortars, enables us to determine that all surface healing in other mortars was due to either the

inclusion of GM, bacterial activity or a combination of both, and was not due to natural carbonation processes during the wetting/drying healing period.

The CTRL specimens contained calcium nitrate and yeast extract directly added to the mortars. Here it was shown that for the uncarbonated mortars there was observable healing at the surface and a good recovery of the water penetration properties. However, the cracks formed in these specimens were smaller than those in other mortars and this may have facilitated healing and it should not be considered that healing would have been of the same degree had the cracks been closer to 0.4 to 0.5 mm in width. When cracks were formed after carbonation, visual observations showed no healing for the CTRL mortars. This suggests that the availability of calcium hydroxide in the uncarbonated mortars must be key in ensuring the autogenous self-healing observed. Clearly, as shown through TGA (Figure 9) the direct addition of calcium nitrate led to greater quantities of calcium hydroxide in the uncarbonated mortars. It is likely that this calcium hydroxide acted as the source of Ca^{2+} ions for effective healing when required. This excess of calcium hydroxide may have aided healing via natural carbonation during the wet/dry healing period. However, as described above, the fact that the REF mortar showed no autogenous healing at the surface at all, despite the availability of some calcium hydroxide, means we can reject this hypothesis. Consequently, it is postulated that the yeast extract allowed some of the environmental bacteria in the healing water to grow in the cracks and that this has led to healing.

4.1.2 Bacteria-based self-healing mortars with direct addition of GM

The CaN-direct mortars used in this research contained spores of *B. cohnii* encapsulated in ACG with the GM added directly to the matrix. It was observed that for these mortars, those that were not carbonated before they were cracked, healed well – both visually in terms of crack reduction (100% crack closure at 84 days) and in recovery of water penetration properties. However, when cracks were formed after carbonation the degree of healing was poor; with only 10% crack closure at 84 days.

For autonomous bacteria-based self-healing to occur in these mortars, Ca^{2+} ions need to be attracted to the surface of the bacteria. As discussed previously, and as for the CTRL specimens, the most accessible form of Ca^{2+} ions is most likely to be calcium hydroxide. Since there was no calcium hydroxide present in the carbonated mortars this explains why healing did not occur. Consequently, it appears that the direct addition of calcium nitrate to mortar is not a practicable means of obtaining self-healing in concrete that is likely to carbonate before it cracks because the Ca^{2+} ions become locked in a form that is insufficiently soluble for the bacteria to use. This observation has not been noted in previous research.

Nevertheless, that these mortars healed well in uncarbonated conditions remains a positive finding. Indeed, it was observed that in the uncarbonated mortars the degree of healing was similar if not better than the degree of healing observed when GM was included in the mortar in an encapsulated form (discussed below). This suggests that sufficient Ca^{2+} was formed within the vicinity of the crack for precipitation of calcium carbonate to take place and consequently it can be argued that the direct addition of GM is a suitable option for self-healing when concrete will not be subject to significant carbonation over its life-time.

4.1.3 Self-healing mortars with encapsulated GM

In both CaN-encap and CaNY-encap the GM was encapsulated in ACG. This prevented the calcium nitrate, therein, from reacting with water to form calcium hydroxide before any cracking occurred and therefore in the carbonation environment it did not convert to calcium carbonate.

It was observed that for these mortars crack closure and a recovery of water-flow resisting properties was observed under both uncarbonated and carbonated conditions. CaN-encap had healing of 81% (crack closure) in uncarbonated conditions and 33% (crack closure) in carbonated conditions; whilst CaNY-encap had a healing ratio of 100% in uncarbonated conditions and 76% in carbonated conditions (Table 2). A similar trend in terms of self-healing capability was observed in the water flow test results (Table 3).

From the observations on the carbonated mortars and comparison with the mortars where GM was added directly (CaN-direct), it can be reasoned that the source of Ca^{2+} ions in these mortars was the encapsulated calcium nitrate. The ability of these mortars to self-heal was related only to the ability of the ACG to fracture and release the GM (calcum nitrate and yeast extract) at the location of the crack. However, noticeably the degree of healing was less than that in uncarbonated mortars. This suggests that in uncarbonated mortars, calcium hydroxide generated by the hydration of cement is also utilised by the bacteria for healing purposes.

It should be noted that after carbonation, the “healing” product at the surface of CaN-encap and CaNY-encap mortars had a gel-like status, and differed from what occurred in the uncarbonated mortars. The most likely explanation is that these gel-like phases are bacterial biofilm or a by-product of the growth of the bacterial cells. This biofilm was mainly formed in the first two months but disappeared by 84 days. Some large crystal precipitates were shown to fill the crack after the disappearance of the biofilm. Based on the water flow test results, and the fact that CaN-encap and CaNY-encap had good recovery of water-flow resistance it is most likely that calcium carbonate was precipitated on the biofilm, providing sufficient healing performance. More of this gel-like formation was observed in the CaNY-encap mortars. This makes sense, because CaNY-encap contained four times as much yeast extract as CaN-encap, would support a marked increase in bacterial biomass and could easily lead to more biofilm formation. The high content of calcium detected by EDX mapping in the area between the original crack surface and the black gel-like healing material suggested that calcite was precipitated here. The most likely explanation for this arrangement is that a bacterial biofilm may form the first layer of the healing process in carbonated CaNY-encap mortars, providing a scaffold and nucleation surface on which calcite can precipitate over time, leading to robust and complete crack healing.

4.1.4 Summary of effect of carbonation on self-healing of mortars

Overall these results make clear that an important source of Ca^{2+} ions for bacteria-based self-healing of cementitious composites is calcium hydroxide, present either as a consequence of hydrolysis or hydration of Portland cement, or from the dissolution of calcium nitrate deliberately added to the cementitious composite during mixing. For cementitious composites that do not carbonate prior to cracking, this calcium hydroxide is sufficient to provide an efficient level of healing. We note that supplying an extra source of Ca^{2+} ions at the moment of cracking, due to encapsulation, enhanced the degree of healing. However, in carbonated cementitious composites calcium hydroxide is not available as a source of Ca^{2+} ions. We here show for the first time that the self-healing of cementitious composites that crack after carbonation is almost totally dependent on the availability of Ca^{2+} ions released from an encapsulated source. Therefore, whilst the direct addition and encapsulation of calcium nitrate are both suitable for providing self-healing of cementitious composites, the conditions of the concrete during service life need to be considered when choosing the most appropriate option. For cementitious composites exposed to XC conditions it is suggested that the calcium source must be encapsulated in the mortar prior to mixing.

4.2 Effect of yeast extract content on self-healing

To ensure sufficient DIC, a carbon source was added to the mortars to aid bacteria-based self-healing. In this research, yeast extract alone was used as the source of DIC to deliver bacteria-based self-healing, something that had not been tried previously.

It was observed that all mortars containing bacteria and yeast extract healed when subject to uncarbonated conditions prior to cracking. Consequently, the results of this work are clear in that yeast extract was able to provide sufficient DIC for the bacteria to promote the precipitation of calcium carbonate.

In both uncarbonated and carbonated mortars it was shown that CaNY-encap was more effective at providing crack closure and recovery of water flow properties than CaN-encap.

548 The only difference between these two mortars was in the quantity of yeast extract added,
549 and in the tests described, yeast extract was the only nutrient source used to aid spore
550 germination and bacterial growth. Since the yeast extract was consumed by the bacteria, its
551 availability diminished with time. It can be deduced that, because CaNY-encap contains a
552 greater quantity of yeast extract, growth of bacteria can take place over a much longer
553 period.
554 Whilst yeast extract was the principle source of DIC, under the wet/dry healing conditions
555 used it is possible that some environmental CO_2 may have ingressed into the mortar.
556 However, since the quantity of DIC is directly related to the amount of CO_3^{2-} ions formed, it
557 remains that the volume of calcium carbonate precipitated is necessarily related to the
558 availability of yeast extract. This may at first glance appear a fairly obvious observation;
559 however research elsewhere has shown that too much yeast extract can inhibit calcium
560 carbonate precipitation [32]. However, unlike in the work described here, the yeast extract
561 there was used in combination with other sources of DIC.
562
563 **5 Conclusions**
564 This research has shown that an important source of Ca^{2+} ions for bacteria-based self-
565 healing of cementitious composites is calcium hydroxide. However, in carbonated
566 cementitious composites calcium hydroxide is not available as a source of Ca^{2+} ions.
567 Consequently, we have shown here for the first time, that bacteria-based self-healing, in
568 cementitious composites that have carbonated prior to cracking, is almost totally dependent
569 on the availability of Ca^{2+} ions released from an encapsulated source.
570 The following specific conclusions can be drawn:
571 1. Coated ACG is an effective medium for encapsulating spores and GM in bacteria-
572 based self-healing cementitious composites. It survives the mixing and hardening
573 process intact, causes no retardation and fractures when cracks are formed.

2. Uncarbonated mortars show higher self-healing efficiency than carbonated mortars. Calcium carbonate precipitates within approximately seven days, and complete surface crack closure can be observed visually in less than a month.
3. In carbonated specimens, where healing is only observed with encapsulated GM, a biofilm was observed to be formed and fill the crack for up to 84 days. Only then did the precipitated calcium carbonate within the crack become visible. It is possible that the formation of a bacterial biofilm contributes to early crack-healing, while calcium carbonate precipitation on the surface of the biofilm over time leads to the crack closure.
4. The quantity of yeast extract available for use by the bacteria governs self-healing performance when bacteria are used with calcium nitrate. The quantity of calcium carbonate that can form is directly related to the amount of yeast extract provided.

ACKNOWLEDGEMENTS

The authors would like to acknowledge EPSRC (Project No. EP/PO2081X/1) and Industrial collaborators/partners for funding the Resilient Materials for Life (RM4L) project. We thank technical staff in the Department of Architecture and Civil Engineering and the Department of Biology and Biochemistry for key support. We further thank colleagues at the Material and Chemical Characterisation Facility (MC^2) at University of Bath (https://doi.org/10.15125/mx6j-3r54) for their assistance with scanning electron microscopy.

REFERENCES

[1] A. Al-Tabbaa, B. Lark, K. Paine, T. Jefferson, C. Litina, D. Gardner, T. Embley, Biomimetic cementitious construction materials for next-generation infrastructure, Proc. Inst. Civ. Eng. - Smart Infrastruct. Constr. (2018) 1–35. doi:https://doi.org/10.1680/jsmic.18.00005.

[2] A. Mignon, G.J. Graulus, D. Snoeck, J. Martins, N. De Belie, P. Dubruel, S. Van Vlierberghe, pH-sensitive superabsorbent polymers: a potential candidate material for

602 self-healing concrete, J. Mater. Sci. 50 (2014) 970–979. doi:10.1007/s10853-014-
603 8657-6.
604 [3] M. Roig-Flores, F. Pirritano, P. Serna, L. Ferrara, Effect of crystalline admixtures on
605 the self-healing capability of early-age concrete studied by means of permeability and
606 crack closing tests, Constr. Build. Mater. 114 (2016) 447–457.
607 doi:10.1016/j.conbuildmat.2016.03.196.
608 [4] L. Souza, A. Kanellopoulos, A. Al-Tabbaa, Production of microcapsules for self-
609 healing concrete using microfluidics, in: 5th Int. Conf. Self-Healing Mater., Durham,
610 USA, 2015.
611 [5] A. Kanellopoulos, P. Giannaros, A. Al-Tabbaa, The effect of varying volume fraction of
612 microcapsules on fresh, mechanical and self-healing properties of mortars, Constr.
613 Build. Mater. 122 (2016) 577–593. doi:10.1016/J.CONBUILDMAT.2016.06.119.
614 [6] R.E. Davies, A. Jefferson, R. Lark, D. Gardner, A novel 2D vascular network in
615 cementitious materials, in: Fib Symp. , Copenhagen, Denmark, 2015.
616 http://orca.cf.ac.uk/86643/ (accessed December 2, 2018).
617 [7] N. De Belie, E. Gruyaert, A. Al-Tabbaa, P. Antonaci, C. Baera, D. Bajare, A.
618 Darquennes, R. Davies, L. Ferrara, T. Jefferson, C. Litina, B. Miljevic, A. Otlewska, J.
619 Ranogajec, M. Roig-Flores, K. Paine, P. Lukowski, P. Serna, J.M. Tulliani, S. Vucetic,
620 J. Wang, H.M. Jonkers, A Review of Self-Healing Concrete for Damage Management
621 of Structures, Adv. Mater. Interfaces. 5 (2018) 1–28. doi:10.1002/admi.201800074.
622 [8] W. De Muynck, N. De Belie, W. Verstraete, Microbial carbonate precipitation in
623 construction materials: A review, Ecol. Eng. 36 (2010) 118–136.
624 doi:10.1016/j.ecoleng.2009.02.006.
625 [9] E. Tziviloglou, V. Wiktor, H.M. Jonkers, E. Schlangen, Bacteria-based self-healing
626 concrete to increase liquid tightness of cracks, Constr. Build. Mater. 122 (2016) 118–
627 125. doi:10.1016/j.conbuildmat.2016.06.080.
628 [10] S.S. Bang, J.K. Galinat, V. Ramakrishnan, Calcite precipitation induced by
629 polyurethane-immobilized Bacillus pasteurii, Enzyme Microb. Technol. 28 (2001) 404–

409. doi:10.1016/S0141-0229(00)00348-3.

[11] H. Chen, C. Qian, H. Huang, Self-healing cementitious materials based on bacteria and nutrients immobilized respectively, Constr. Build. Mater. 126 (2016) 297–303. doi:10.1016/J.CONBUILDMAT.2016.09.023.

[12] N. De Belie, J. Wang, Z.B. Bundur, K. Paine, Bacteria-based concrete, in: Eco-Efficient Repair Rehabil. Concr. Infrastructures, Woodhead Publishing, 2018: pp. 531–567. doi:10.1007/978-1-4939-6881-7.

[13] B.J. Reeksting, T.D. Hoffmann, L. Tan, K. Paine, S. Gebhard, In-depth profiling of calcite precipitation by environmental bacteria reveals fundamental mechanistic differences with relevance to application, Appl. Environ. Microbiol. 86 (2020) 1–16. doi:10.1128/aem.02739-19.

[14] J.Y. Wang, H. Soens, W. Verstraete, N. De Belie, Self-healing concrete by use of microencapsulated bacterial spores, Cem. Concr. Res. 56 (2014) 139–152. doi:10.1016/j.cemconres.2013.11.009.

[15] M. Luo, C.X. Qian, Performance of Two Bacteria-Based Additives Used for Self-Healing Concrete, J. Mater. Civ. Eng. 28 (2016) 04016151. doi:10.1061/(ASCE)MT.1943-5533.0001673.

[16] D. Palin, V. Wiktor, H.M. Jonkers, A bacteria-based bead for possible self-healing marine concrete applications, Smart Mater. Struct. 25 (2016) 084008. doi:10.1088/0964-1726/25/8/084008.

[17] M. Alazhari, T. Sharma, A. Heath, R. Cooper, K. Paine, Application of expanded perlite encapsulated bacteria and growth media for self-healing concrete, Constr. Build. Mater. 160 (2018) 610–619. doi:10.1016/j.conbuildmat.2017.11.086.

[18] M. Fahimizadeh, A.D. Abeyratne, L.S. Mae, R. Singh, P. Pasbakhsh, Biological concrete self-healing by hydrogel- immobilized non-ureolytic bacteria, n.d.

[19] J. Xu, X. Wang, Self-healing of concrete cracks by use of bacteria-containing low alkali cementitious material, Constr. Build. Mater. 167 (2018) 1–14. doi:10.1016/J.CONBUILDMAT.2018.02.020.

[20] Z. Başaran Bundur, S. Bae, M.J. Kirisits, R.D. Ferron, Biomineralization in Self-Healing Cement-Based Materials: Investigating the Temporal Evolution of Microbial Metabolic State and Material Porosity, J. Mater. Civ. Eng. 29 (2017) 04017079. doi:10.1061/(ASCE)MT.1943-5533.0001838.

[21] J.L. Zhang, C.G. Wang, Q.L. Wang, J.L. Feng, W. Pan, X.C. Zheng, B. Liu, N.X. Han, F. Xing, X. Deng, A binary concrete crack self-healing system containing oxygen-releasing tablet and bacteria and its Ca2+-precipitation performance, Appl. Microbiol. Biotechnol. 100 (2016) 10295–10306. doi:10.1007/s00253-016-7741-z.

[22] M. Ksara, R. Newkirk, S.K. Langroodi, F. Althoey, C.M. Sales, C.L. Schauer, Y. Farnam, Microbial damage mitigation strategy in cementitious materials exposed to calcium chloride, Constr. Build. Mater. 195 (2019) 1–9. doi:10.1016/j.conbuildmat.2018.10.033.

[23] J.L. Zhang, R.S. Wu, Y.M. Li, J.Y. Zhong, X. Deng, B. Liu, N.X. Han, F. Xing, Screening of bacteria for self-healing of concrete cracks and optimization of the microbial calcium precipitation process, Appl. Microbiol. Biotechnol. 100 (2016) 6661–6670. doi:10.1007/s00253-016-7382-2.

[24] B. Šavija, M. Luković, Carbonation of cement paste: Understanding, challenges, and opportunities, Constr. Build. Mater. 117 (2016) 285–301. doi:10.1016/j.conbuildmat.2016.04.138.

[25] J. Wang, A. Mignon, D. Snoeck, V. Wiktor, S. Van Vliergerghe, N. Boon, N. De Belie, Application of modified-alginate encapsulated carbonate producing bacteria in concrete: a promising strategy for crack self-healing, Front. Microbiol. 6 (2015) 1–14. doi:10.3389/fmicb.2015.01088.

[26] H.M. Jonkers, A. Thijssen, G. Muyzer, O. Copuroglu, E. Schlangen, H.M. Jonkers, A. Thijssen, G. Muyzer, O. Copuroglu, E. Schlangen, Application of bacteria as self-healing agent for the development of sustainable concrete, Ecol. Eng. 36 (2010) 230–235. doi:10.1016/j.ecoleng.2008.12.036.

[27] R. Alghamri, A. Kanellopoulos, A. Al-Tabbaa, Impregnation and encapsulation of

lightweight aggregates for self-healing concrete, Constr. Build. Mater. 124 (2016) 910–921. doi:10.1016/j.conbuildmat.2016.07.143.

[28] RILEM, Measurement of Water Absorption Under Low Pressure. RILEM Test Method No. 11.4, 1987.

[29] J.N. Cernica, Geotechnical Engineering: Soil Mechanics, Wiley, 1995.

[30] X. Chen, J. Yuan, M. Alazhari, Effect of Microbiological Growth Components for Bacteria-Based Self-Healing on the Properties of Cement Mortar, Materials (Basel). 12 (2019). doi:10.3390/ma12081303.

[31] A. Amiri, Z.B. Bundur, Impact of Biogenic Self-Healing Additive on Performance of Cement-Based Mortar, Int. RILEM Conf. Mater. Syst. Struct. Civ. Eng. Conf. Segm. Serv. Life Cem. Mater. Struct. (2016) 493–502.

[32] J. Zhang, B. Mai, T. Cai, J. Luo, W. Wu, B. Liu, N. Han, F. Xing, X. Deng, Optimization of a Binary Concrete Crack Self-Healing System Containing Bacteria and Oxygen, Materials (Basel). 10 (2017) 116. doi:10.3390/ma10020116.

Supplementary documents:

1. XRD
2. Crack closure progression photos
3. SEM and EDX images across cracks of selected mortars

1. **XRD**

An accelerated carbonation method was used in this work to convert the calcium hydroxide formed during the hydrolysis and hydration of cement to calcium carbonate prior to cracking to test the effects of this on self-healing. As shown by the TGA and XRD results this was successful and after carbonation there was no calcium hydroxide present in either the REF or CTRL mortars.

The analyses show some items of interest. Firstly, there was no evidence of ettringite in the carbonated REF mortars. Ettringite is known to carbonate to form calcium carbonate, gypsum ($CaSO_4.2H_2O$), alumina gel ($Al_2O_3.H_2O$) and water [31]. Indeed, the presence of gypsum in carbonated REF mortars was identified. In contrast, the quantity of ettringite in the carbonated CTRL mortars was similar to the uncarbonated mortar and no gypsum was formed. This may be because the addition of calcium nitrate caused an increase in calcium hydroxide content, and subsequently during the timeframe of the carbonation period CO2 was largely consumed by calcium hydroxide

Figure S1 shows the XRD results of uncarbonated and carbonated REF and CTRL paste samples.

(a)

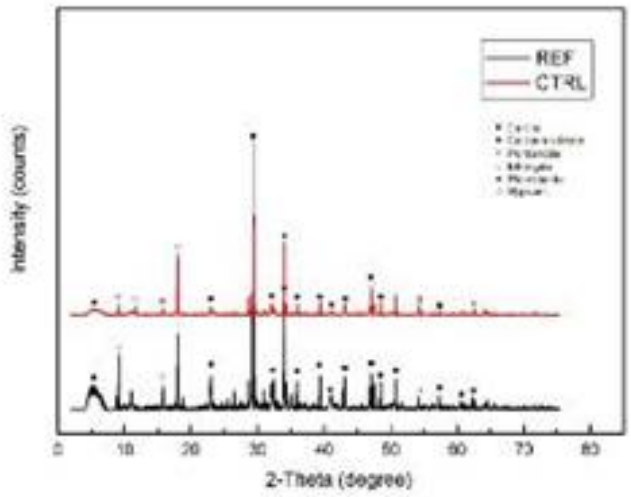

(b)

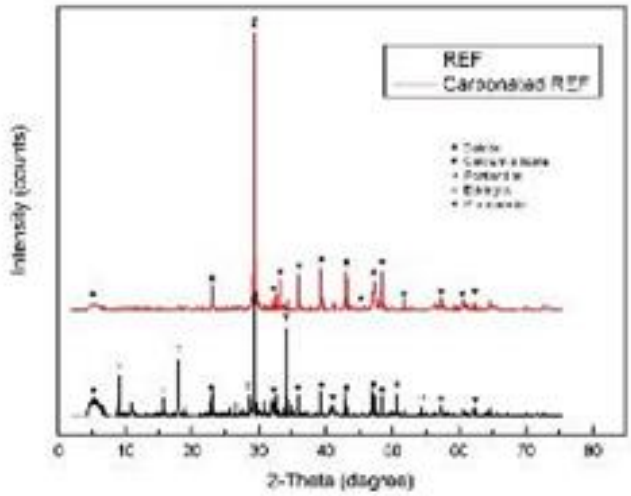

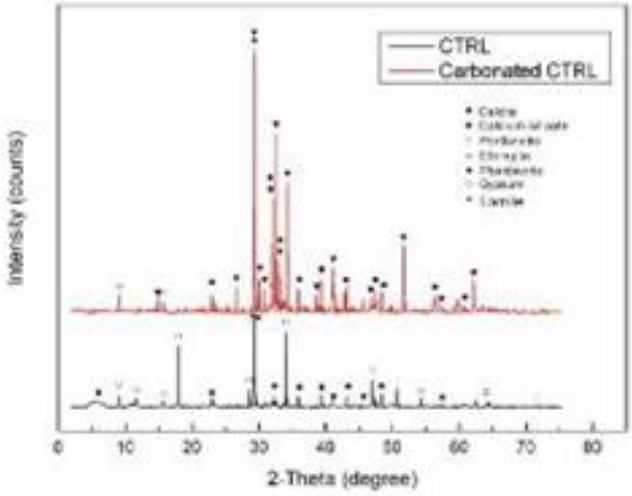

Figure S1 XRD results of (a) REF & CTRL, (b) REF & carbonated REF and (c) CTRL and carbonated CTRL

727

2. Crack Closure Progression

Progression photos of crack healing of each mortar are shown in Figure S2-6

(a)

(b)

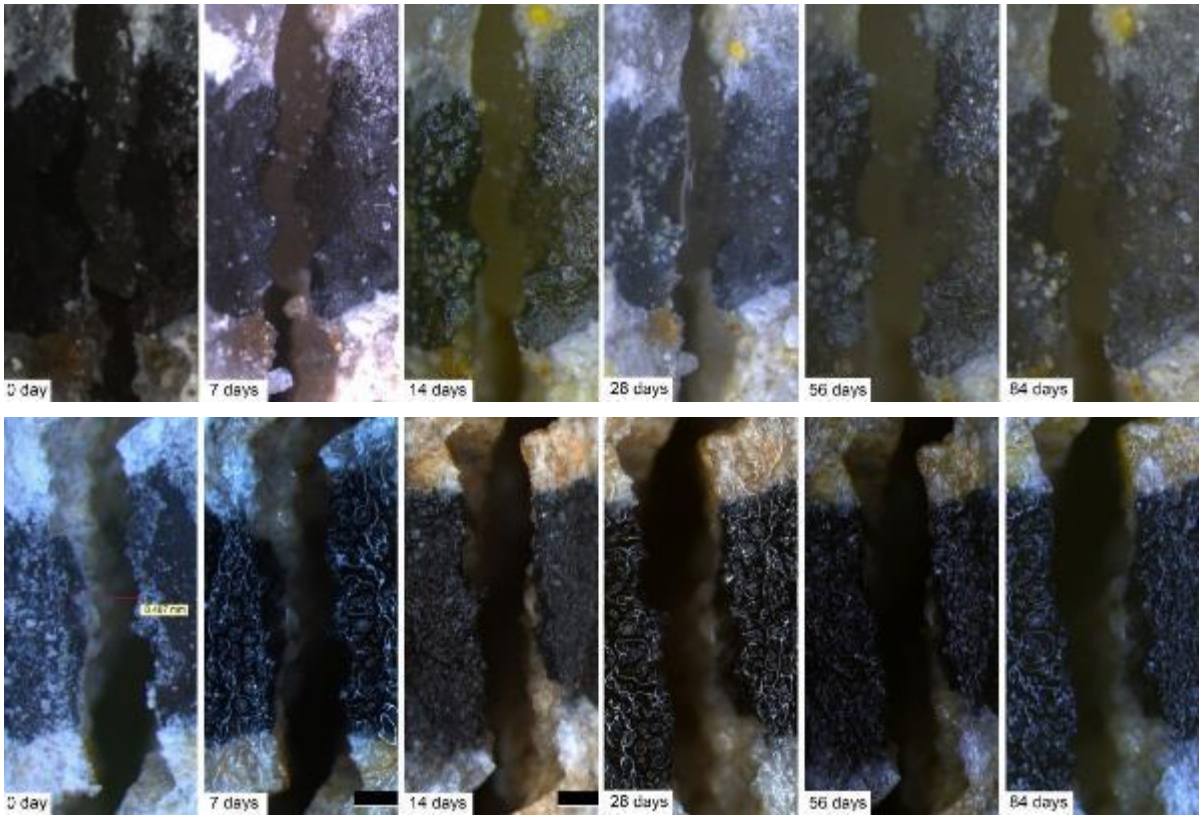

Figure S3 Progression of crack healing in (a) REF and (b) carbonated REF

(a)

(b)

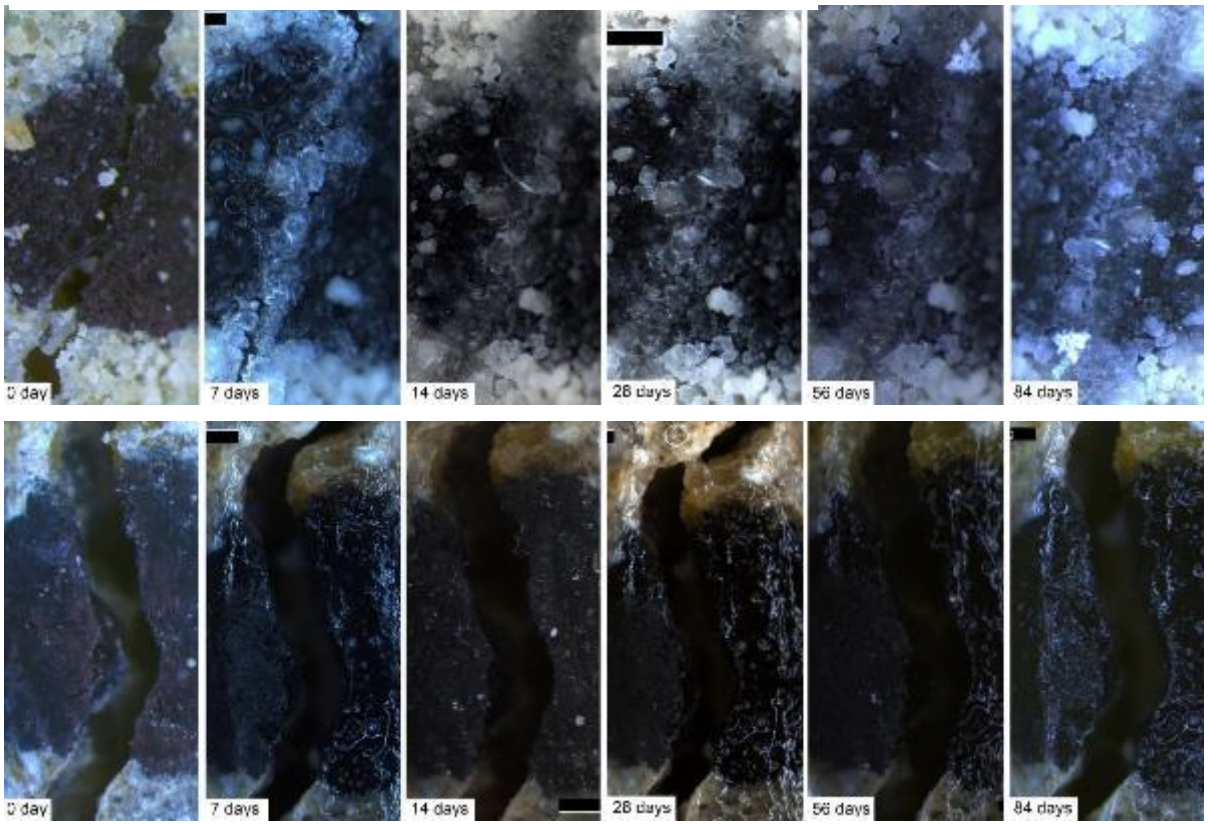

Figure S2 Progression of crack healing in (a) CTRL and (b) carbonated CTRL

731

(a)

(b)

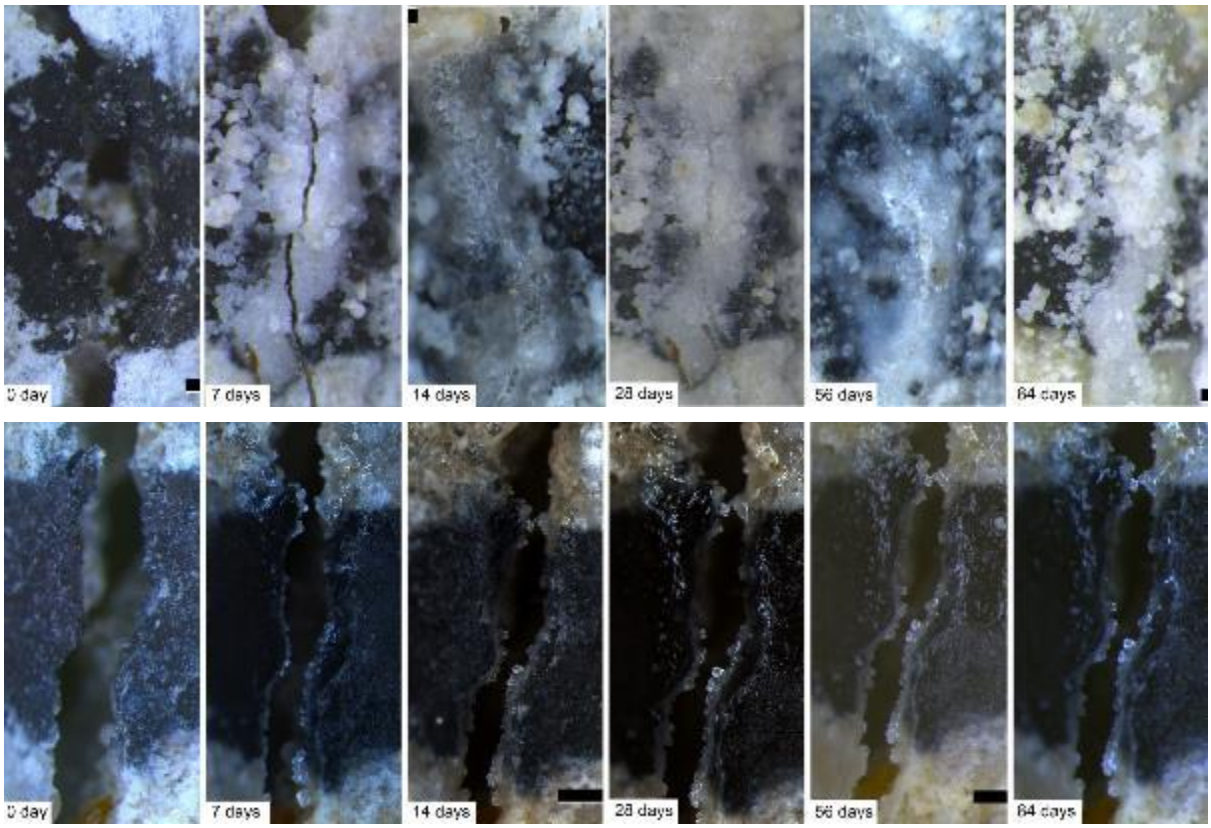

Figure S5 Progression of crack healing in (a) CaN-direct and (b) carbonated CaN-direct

732

(a)

(b)

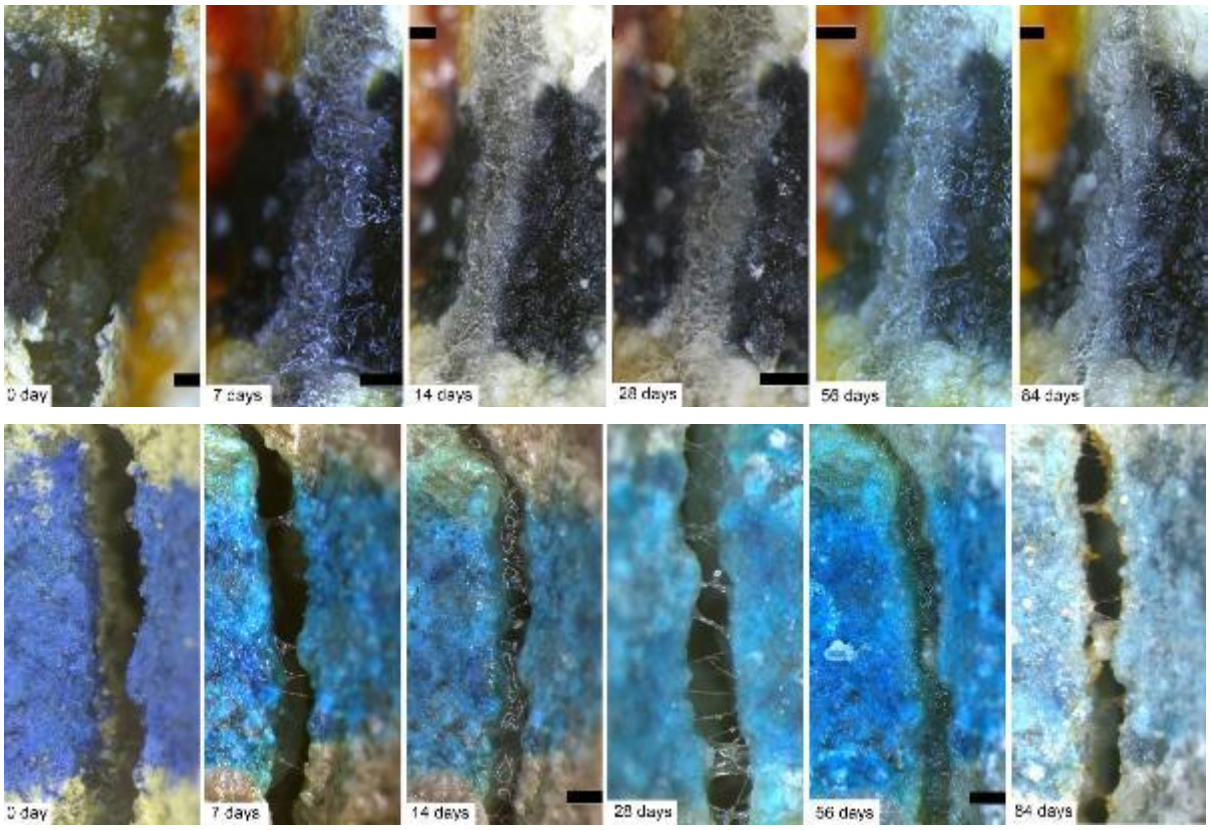

Figure S4 Progression of crack healing in (a) CaN-encap and (b) carbonated CaN-encap

733

(a)

(b)

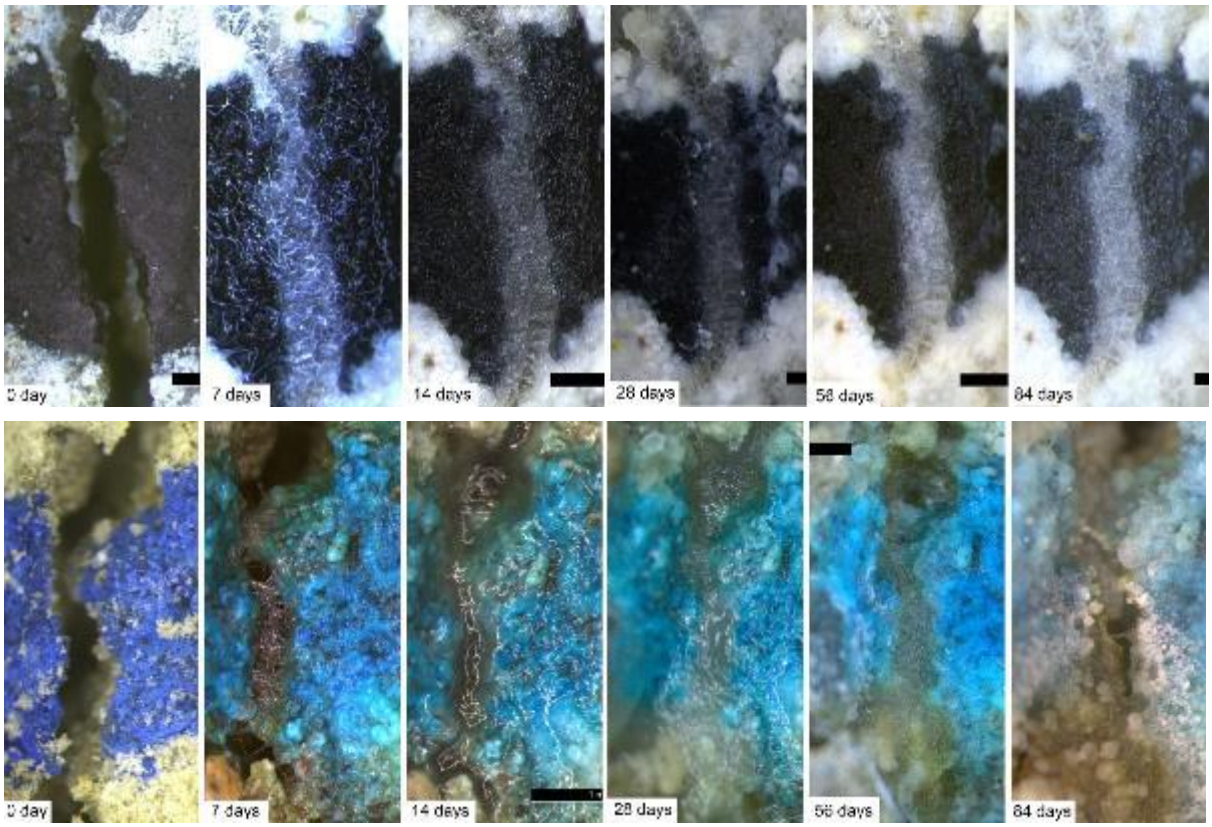

Figure S6 Progression of crack healing in (a) CaNY-encap and (b) carbonated CaNY-encap

3. SEM and EDX images across cracks of selected mortars

SEM images and XRD results of uncarbonated CTRL, uncarbonated CaN-direct, uncarbonated CaN-encap, uncarbonated CaNY-encap and carbonated CaNY-encap are shown in Figure S7-11. EDX values are included for completeness but due to the nature of the techniques used the values for C and O are of limited practical application.

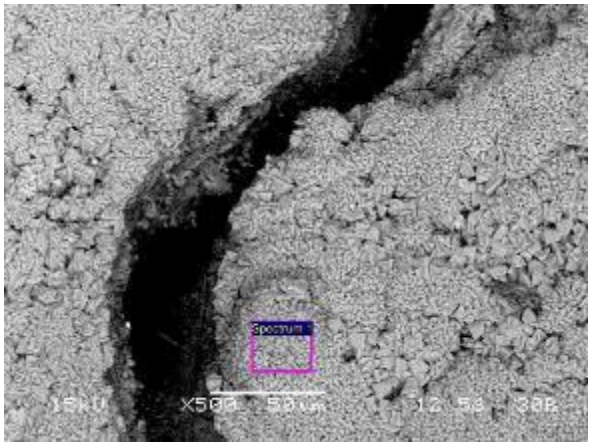

(a)

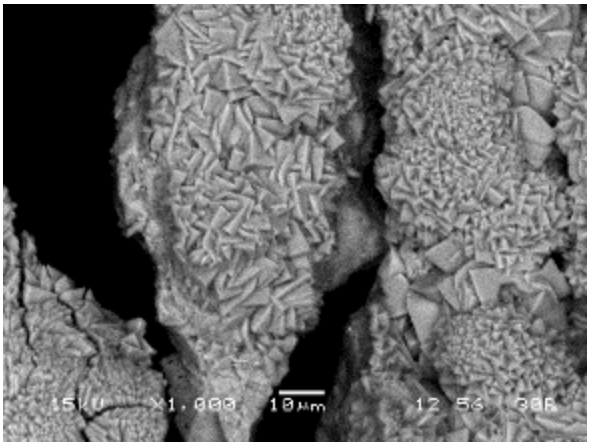

(b)

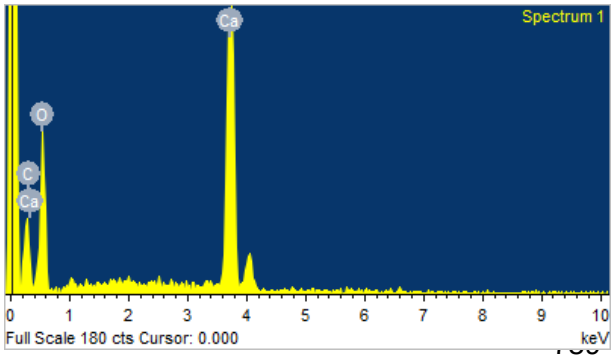

Element	Weight%	Atomic%
C K	13.26	21.42
O K	50.25	60.92
Ca K	36.49	17.66
Totals	100.00	

Figure S7 SEM and EDX of uncarbonated CTRL

763

764

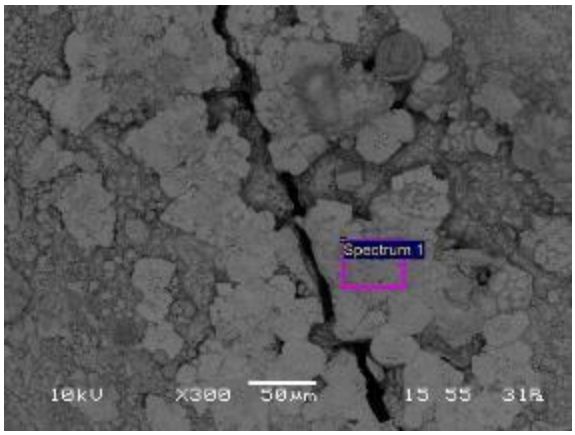

(a)

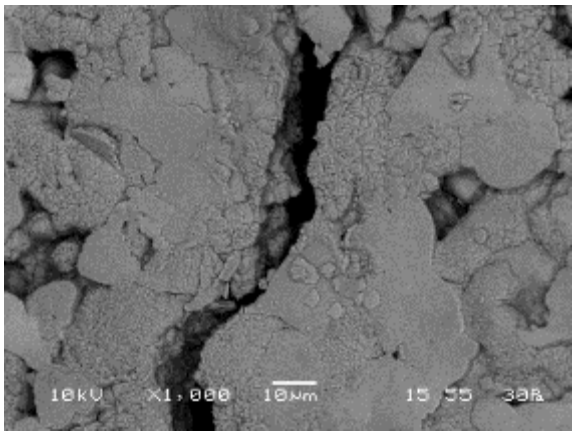

(b)

765

766

767

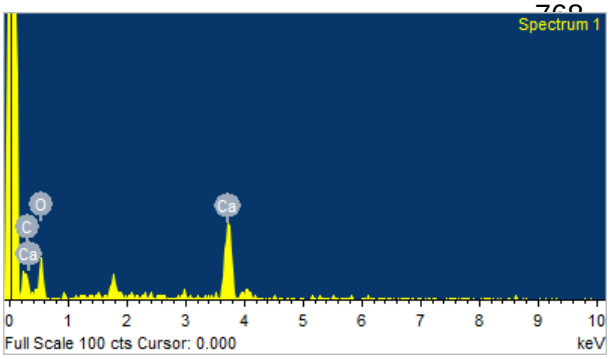

Element	Weight%	Atomic%
C K	10.48	18.75
O K	41.16	55.30
Ca K	48.37	25.94
Totals	100.00	

771

Figure S8 SEM and EDX of uncarbonated CaN-direct

72

. 73

774

775

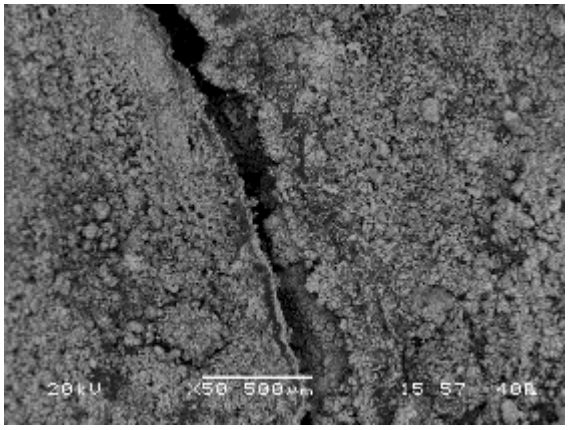

(a)

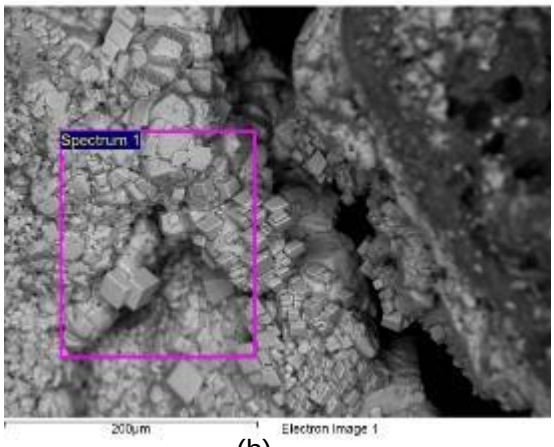

(b)

776

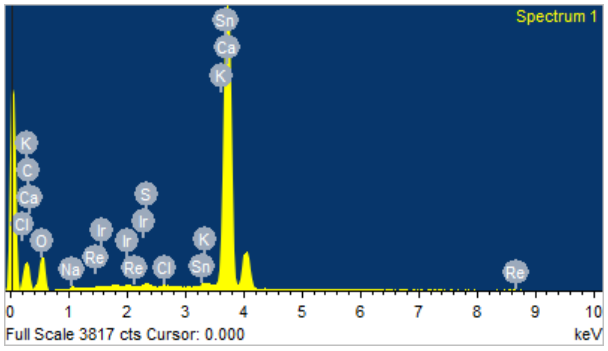

Figure S9 SEM and EDX of uncarbonated CaN-encap

Element	Weight%	Atomic%
C K	24.78	39.35
O K	35.15	41.90
Na K	0.30	0.25
S K	0.29	0.17
Cl K	0.13	0.07
K K	0.50	0.25
Ca K	37.41	17.80
Sn L	1.10	0.18
Ir M	0.34	0.03
Totals	100.00	

777

778

779

780

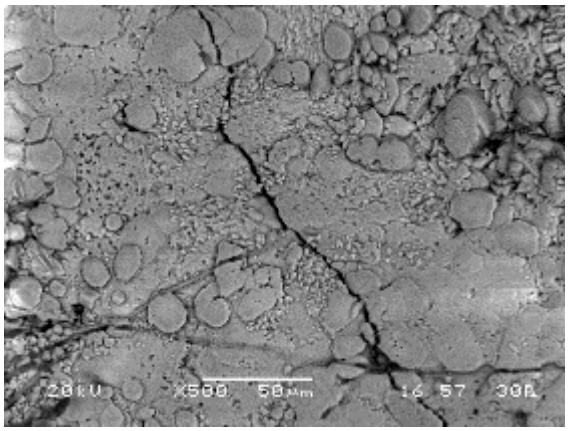

(a)

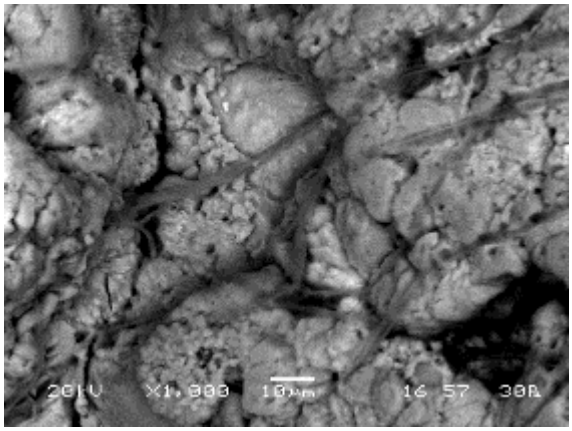

(b)

781

782

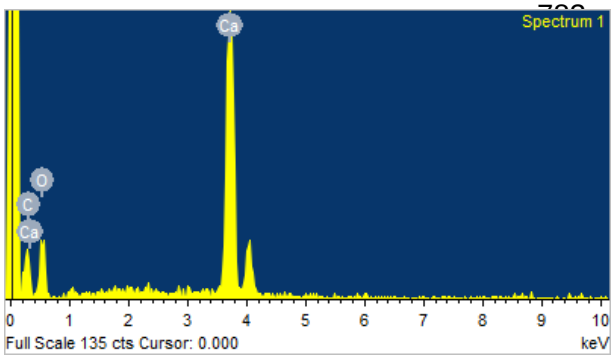

Element	Weight%	Atomic%
C K	25.74	38.70
O K	41.06	46.34
Ca K	33.20	14.96
Totals	100.00	

Figure S10 SEM and EDX of uncarbonated CaNY-encap

787

788

789

790

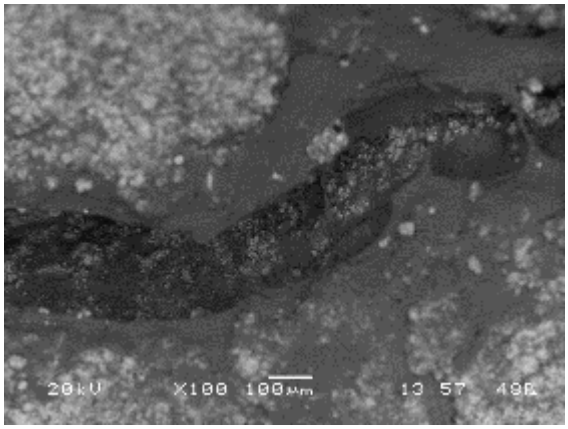

(a)

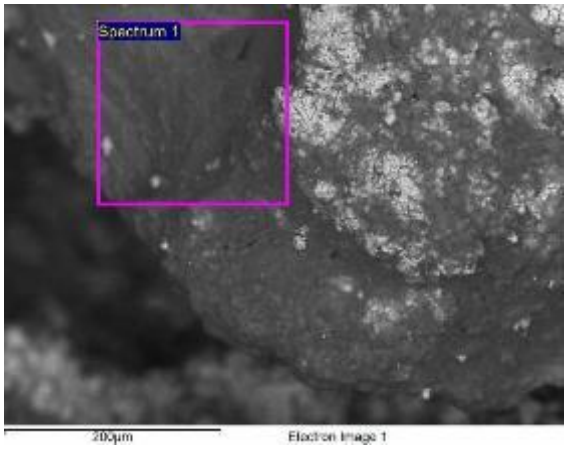

(b)

791

792

793

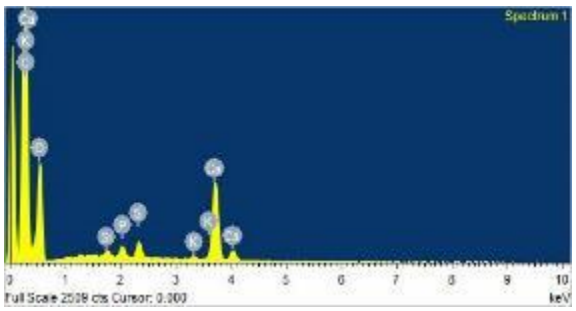

Figure S11 SEM and EDX of carbonated CaNY-encap

Element	Weight%	Atomic%
C K	60.76	69.29
O K	33.41	28.60
Si K	0.18	0.09
P K	0.43	0.19
S K	0.65	0.28
K K	0.14	0.05
Ca K	4.43	1.51
Totals	100.00	

795

796

797 4.2.1